Acta Geochim (2025) 44:994–1013
https://doi.org/10.1007/s11631-025-00756-z

ORIGINAL ARTICLE

Geochemistry of the siliciclastic sediments from the Raniganj Gondwana basin, West Bengal, India, and its geological implications

Y. Priyananda Singh[1] · Oinam Kingson[2] · K. Milankumar Sharma[3] · Raghavendra Prasad Tiwari[1] · Rajeev Patnaik[4] · Prosenjit Ghosh[5] · Anupam Sharma[6] · Jitendra Kumar Pattanaik[1] · Pankaj Kumar[7] · Harel Thomas[8] · Ningthoujam Premjit Singh[9] · Prem Chand Kisku[10] · N. Amardas Singh[1]

Received: 12 August 2024 / Revised: 3 January 2025 / Accepted: 7 January 2025 / Published online: 11 February 2025

Abstract Elemental concentrations of the siliciclastic sediments from a sedimentary basin provide clues on paleo-weathering, paleoclimate, provenance, and tectonic setting of the basin. Records for Permo–Triassic mass extinction and climatic fluctuations are commonly traced from the sediments in the Gondwana basins. Nevertheless, our understanding on sedimentation, provenance, and regional tectonics of the Raniganj Basin, a Gondwana basin in the eastern India is poor. Minerals including clay particles and major and trace element concentrations of the siliciclastic sediments from different formations of the Raniganj Basin have been studied to establish the paleo-weathering, paleoclimate, provenance, and tectonic settings of the basin. This study suggests that the Talchir Formation experienced cold and dry climatic conditions at the sediment source area, while the Barakar, Raniganj, and Panchet formations had prevailing semiarid climates. The sources of the siliciclastic sediments are from the felsic rocks of the Chotanagpur Granite Gneissic Complex (CGGC). Further, the geochemical results suggest a rift-like (passive) tectonic setting for the Raniganj Basin, while few samples represent the collision tectonic setting of the basement CGGC, formed due to collision of major Indian blocks during the Paleo-Neoproterozoic time.

Supplementary Information The online version contains supplementary material available at https://doi.org/10.1007/s11631-025-00756-z.

✉ K. Milankumar Sharma
milankumar.sharma@gmail.com

Y. Priyananda Singh
priyananda1234@gmail.com

Oinam Kingson
kingsonoinam39@gmail.com

Raghavendra Prasad Tiwari
rptmzu@rediffmail.com

Rajeev Patnaik
rajeevpatnaik@gmail.com

Prosenjit Ghosh
pghosh@iisc.ac.in

Anupam Sharma
anupam110367@gmail.com

Jitendra Kumar Pattanaik
jitendra.bapi@gmail.com

Pankaj Kumar
baghelpankaj@gmail.com

Harel Thomas
harelthomas@gmail.com

Ningthoujam Premjit Singh
ningthoujampremjit11@gmail.com

Prem Chand Kisku
premchkisku@gmail.com

N. Amardas Singh
nongmaithemamardassingh@hotmail.com

[1] Department of Geology, Central University of Punjab, VPO Guddah, Bathinda 151401, India

[2] Department of Geology, Banaras Hindu University, Varanasi 221005, India

[3] Department of Geology, Central University of South Bihar, Gaya 824236, India

[4] Department of Geology, Panjab University, Chandigarh 160014, India

[5] Centre for Earth Sciences, Indian Institute of Science, Bengaluru 560012, India

[6] Birbal Sahni Institute of Palaeoscience, Lucknow 226007, India

[7] Inter-University Accelerator Centre (IUAC), New Delhi 110067, India

Keywords Siliciclastic sediments · Geochemistry · Paleoclimate · Provenance · Tectonic setting · Raniganj Basin

1 Introduction

The geochemical composition of siliciclastic sediments provides important information on the factors that regulate weathering and erosion through the geologic age. Worldwide, many studies have used geochemical data to interpret paleo-weathering, paleoclimate, provenance, tectonic settings, and evolution of a basin (Wanas and Abdel-Maguid 2006; Ghosh and Sarkar 2010; Ghosh et al. 2012; Garzanti et al. 2014; Garzanti and Resentini 2016; Sawant et al. 2017; Armstrong-Altrin et al. 2019; Wanas and Assal 2021; Singh et al. 2022; Sangeeta et al. 2023; Abdulfarraj et al. 2024). The sedimentation in the Gondwana Basin has recorded the signature of the Late Paleozoic Ice Age and biotic evolution along with a transition in global climate from the cold ice house during the Permo-Carboniferous to the wet greenhouse climate of the Cretaceous (Fielding et al. 2008; Isbell et al. 2012). The Gondwana basins of peninsular India existed between the Gondwana basins of Australia and Africa during the Permian/Triassic (P/T) time, evidenced by Pangean reconstruction (Sarkar et al. 2003). The Raniganj Basin, a sub-basin of the Gondwana Basin of peninsular India, hosts an approximately 2000-m-thick sedimentary rock succession of the Gondwana Supergroup (Late Carboniferous to Early Cretaceous; Ghosh et al. 1996). The sedimentation of the Raniganj Basin partly covers the P/T mass extinction in which ~ 70% of terrestrial and ~ 81% of the marine life at the species level perished (Algeo et al. 2015; Chen et al. 2014; Fan et al. 2020).

The global catastrophe of the P/T event created a global disruption in environmental and geomorphic settings that also induced changes in sedimentation of the basins (Cui et al. 2017; Zhu et al. 2019; Jurikova et al. 2020). Previous studies commonly referred to the Permo–Triassic marine environmental settings (Algeo et al. 2011; Nabbefeld et al. 2010; Shen et al. 2016; Zhang et al. 2018). Therefore, it is equally important to study terrestrial environments like the Raniganj Basin.

Reports with detailed geochemical analysis of siliciclastic sediments from the Raniganj Basin are sparse and have not been available for entire formations of the basin (Pascoe 1956; Dutta 1983; Suttner and Dutta 1986; Sarkar et al. 2003; Bhattacharjee et al. 2018; Ghosh et al. 2019). The organic carbon isotope data of the sediments from the Raniganj Basin, India, recorded around 9‰ fall in the $\delta^{13}C$ values during the Early Triassic across Pangea (Sarkar et al. 2003), resulting in a climatic shift from humid to warm semi-arid type and extinction of terrestrial plants (Sarkar et al. 2003). The major element analysis of the clastic sediments in the Barakar Formation, Raniganj Basin suggests an immature, moderate to strong chemical weathering under warm climatic conditions and support a passive continental–marine marginal setting (Bhattacharjee et al. 2018). However, the sedimentation after the late-Paleozoic ice age in the Gondwana basins had recorded fluvial sedimentation globally (Ghosh, and Sarkar 2010; Ghosh et al. 2012; Singh et al. 2022). Pascoe (1956) and Dutta (1983) also suggested that the Chotanagpur Granite Gneissic Complex (CGGC) likely supplied the sediments of the Raniganj Basin. The fission track dating of the apatite also supported the inferred hypothesis that the Raniganj and Panchet formation sediments were derived from the CGGC (Patel et al. 2014).

Since the geochemical studies in earlier works focus only on one or two formations of the Raniganj Basin (Pascoe 1956; Dutta 1983; Suttner and Dutta 1986; Sarkar et al. 2003; Bhattacharjee et al. 2018; Ghosh et al. 2019), a holistic approach is required to understand the variations in the paleo-weathering, paleoclimate, provenance, and tectonic settings during deposition of different formations in the Raniganj Basin. Therefore, the present work aims to reconstruct the provenance, tectonic setting, paleoclimate, and paleo-weathering of the different formations in the Raniganj Basin. To fulfil these aims, a comprehensive mineralogical–geochemical study has been carried out in the siliciclastic sediments of the studied formations of the Raniganj Basin.

2 Geological setting

Raniganj Basin is an intra-cratonic basin in which the Talchir Formation unconformably overlies the CGGC. The basin forms within the Son-Damodar Valley lineament in eastern peninsular India. The geological map of this basin is illustrated in Fig. 1, showing all the sample locations. The Talchir Formation was deposited in glacio-lacustrine environments (Suttner and Dutta 1986). The Talchir Formation is conformably overlain by the Barakar Formation which is characterized by braided to fluvio-lacustrine alluvial deposits (Suttner and Dutta 1986; Ghosh et al. 1996). The Barren Measures Formation is conformably overlain by the Barakar Formation and was deposited in a lacustrine environment (Ghosh 2002). The Upper Permian Raniganj Formation underlies the Barren Measures Formation (Ghosh et al. 1996; Mukhopadhyay et al. 2010). The Lower Triassic Panchet Formation overlies the Raniganj Formation (Suttner and Dutta 1986; Ghosh et al. 1996; Sharma et al. 2024). The litho-sections and descriptions

[8] Department of Applied Geology, Dr. Harisingh Gour Vishwavidyalay, Sagar 470003, India

[9] Biostratigraphy Division, Wadia Institute of Himalayan Geology, Dehradun 248171, India

[10] Geochronology Division, CSIR-National Geophysical Research Institute (NGRI), Hyderabad 500007, India

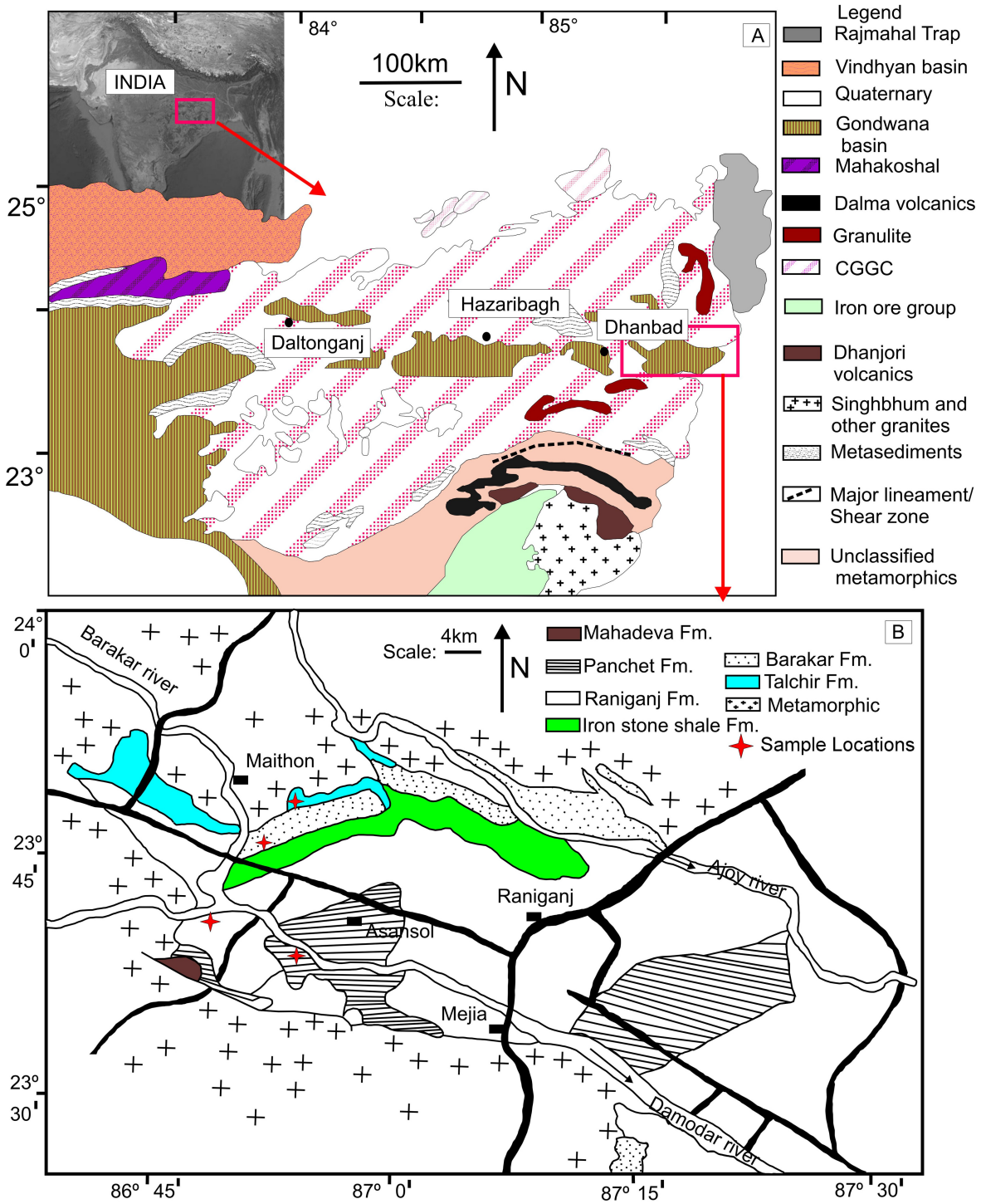

Fig. 1 **A** Map of India showing the location of the basement CGGC along with the Raniganj Basin (modified after Acharyya 2003). **B** Geological map of the Raniganj Basin depicting different formations of the Raniganj Basin (modified after Murthy et al. 2010). The red stars show the sample locations. Fm. formation

on stratigraphic successions of the different formations in the Raniganj Basin are shown in Fig. 2 and Supplementary material 1, respectively.

The CGGC in the eastern part of the Central Indian Tectonic Zone is formed by the continent–continent collision of major Indian blocks during Paleo-Neoproterozoic time (e.g., Acharyya 2003; Bhowmik et al. 2012). The North

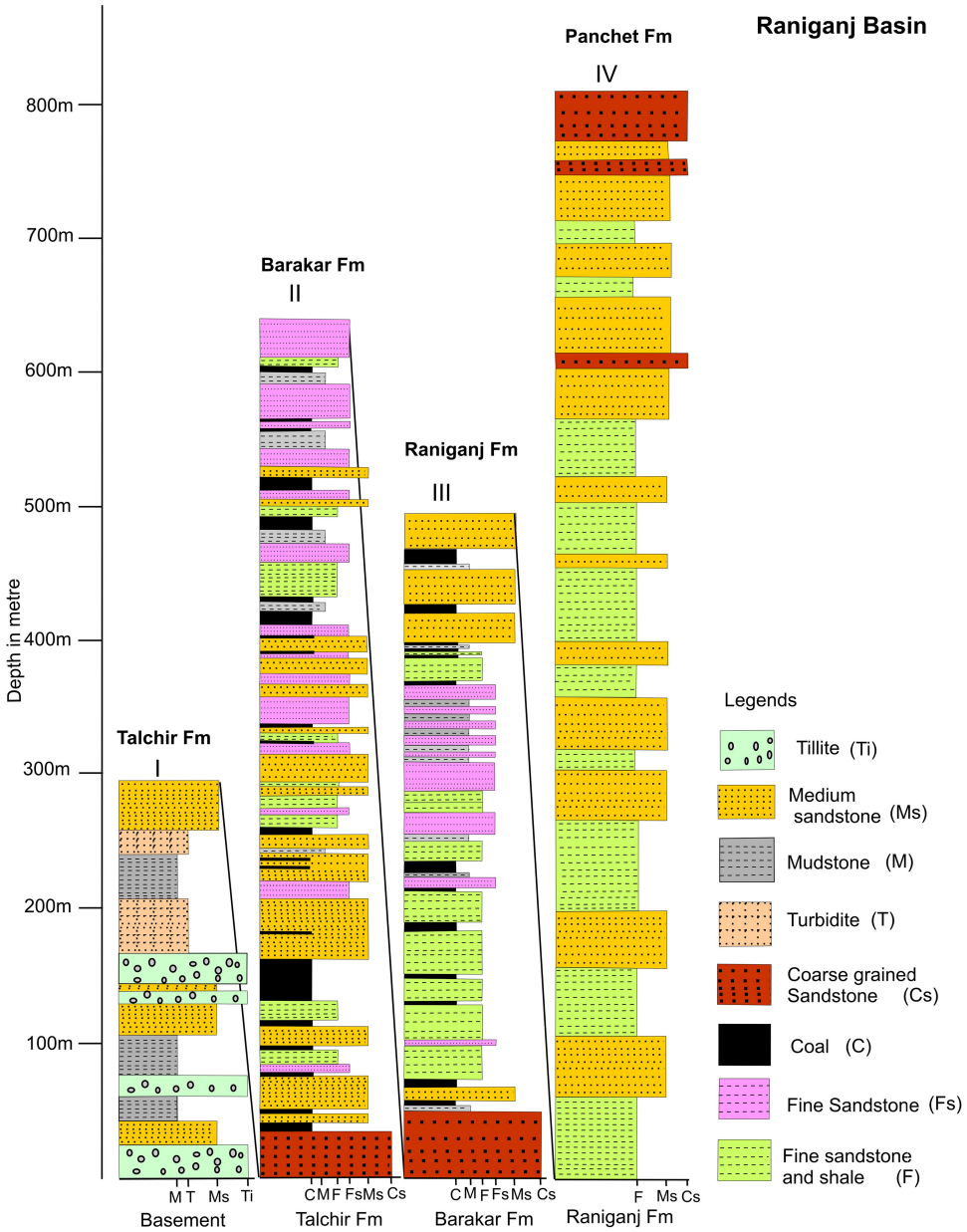

Fig. 2 Lithosection of different formations in the Raniganj Basin; thickness is presented in meters (m). (I) Talchir Formation (from Banerjee 1966), (II) Barakar Formation (after Laskar 1979), (III) Raniganj Formation (from Mehta 1956), and (IV) Panchet Formation (after Casshyap 1979)

Singhbhum Fold Belt separates Archaean Singhbhum Craton from the southern CGGC (Fig. 1). The charnockites and porphyritic granitoids constituted as major rock types of the CGGC, while there were enclaves of khondalites, mafic granulites, calc-silicates, and minor quartzite (Sanyal and Sengupta 2012). The CGGC is traversed by several mafic dykes, such as amphibolitic dykes, gneissic amphibolites, and some doleritic dykes (Ghose et al. 2005). The dykes are considered to be of Precambrian age as they do not traverse through the overlying Gondwana deposits (Mahadevan 2002). The Bengal anorthosite is located in the south-eastern part of the CGGC (Chatterjee et al. 2008).

3 Methodology

3.1 Petrography

Twelve sandstone samples were thin-sectioned and studied for mineralogical and textural analyses using a high-resolution trinocular polarizing microscope (Leica DM750) at the BIOPS-Lab, Department of Geology, Central University of Punjab, Bathinda.

3.2 Clay mineral analysis

Thirty clay samples from the Raniganj Basin were employed to analyze clay minerals. To prepare oriented clay fractions,

standard sample processing and pretreatment techniques as per Deepthy and Balakrishnan (2005) were used. Organic matters were removed from the dis-aggregated samples by treating them with distilled water and H_2O_2, and the samples were finally cleaned. The settling technique (Hardy and Tucker 1988) was applied to the bulk samples for taking out the clay fraction (< 2 µm). Two oriented slides, Ca^{2+} ion-saturated clay slides and K^+ ion-saturated clay slides, were made from each clay sample. Clay mineral slides were scanned by the Empyrean PANalytical X-ray diffractometer housed at the IUAC (Inter-University Accelerator Center), New Delhi, India, operating at 40 mA and 45 kV, equipped with a copper anode. The oriented clay slides were scanned from 2° to 30° 2θ with a scan speed of 0.6° 2θ/min and step size of 0.02° 2θ. Ca-saturated samples were examined under both air-drying and ethylene-glycol-drying conditions. K-saturated samples were scanned at room temperature after being heated at 110 °C, 300 °C, and 550 °C.

The identification of the clay fractions followed Moore and Reynolds' method (1989). The X-ray diffraction (XRD) patterns of different samples from the Raniganj Basin are shown in Fig. 3. Smectite peaks of air-dried samples are identified by a (001) plane having 14.03 Å d-spacing, while the peak changed to ~ 16.7 Å after glycol drying (see Supplementary material 2). In normal air-dried conditions, illite mineral shows 10.0 Å peaks of (001), but in the K-saturated sample, the peak of illite becomes acute on heating to 550 °C. Kaolinite peak displays at 7.2 Å peaks (001), and it disappeared at 550 °C in the K-saturated samples. The clay fraction of gibbsite is identified by the 4.8 Å peak that becomes intense for K-saturated samples, and the peak disappears after heating (300 °C). The goethite clay fraction is confirmed by the 4.1 Å peak. This study has used the semi-quantification formula as given below (Deepthy and Balakrishnan 2005). The peak areas for the clay minerals used in the calculation are determined using X'Pert HighScore Plus software.

$$\text{Clay mineral } \% = 100 \times \left[I_{\text{clay mineral}} / \Sigma I_{\text{all clay minerals in the sample}}\right],$$

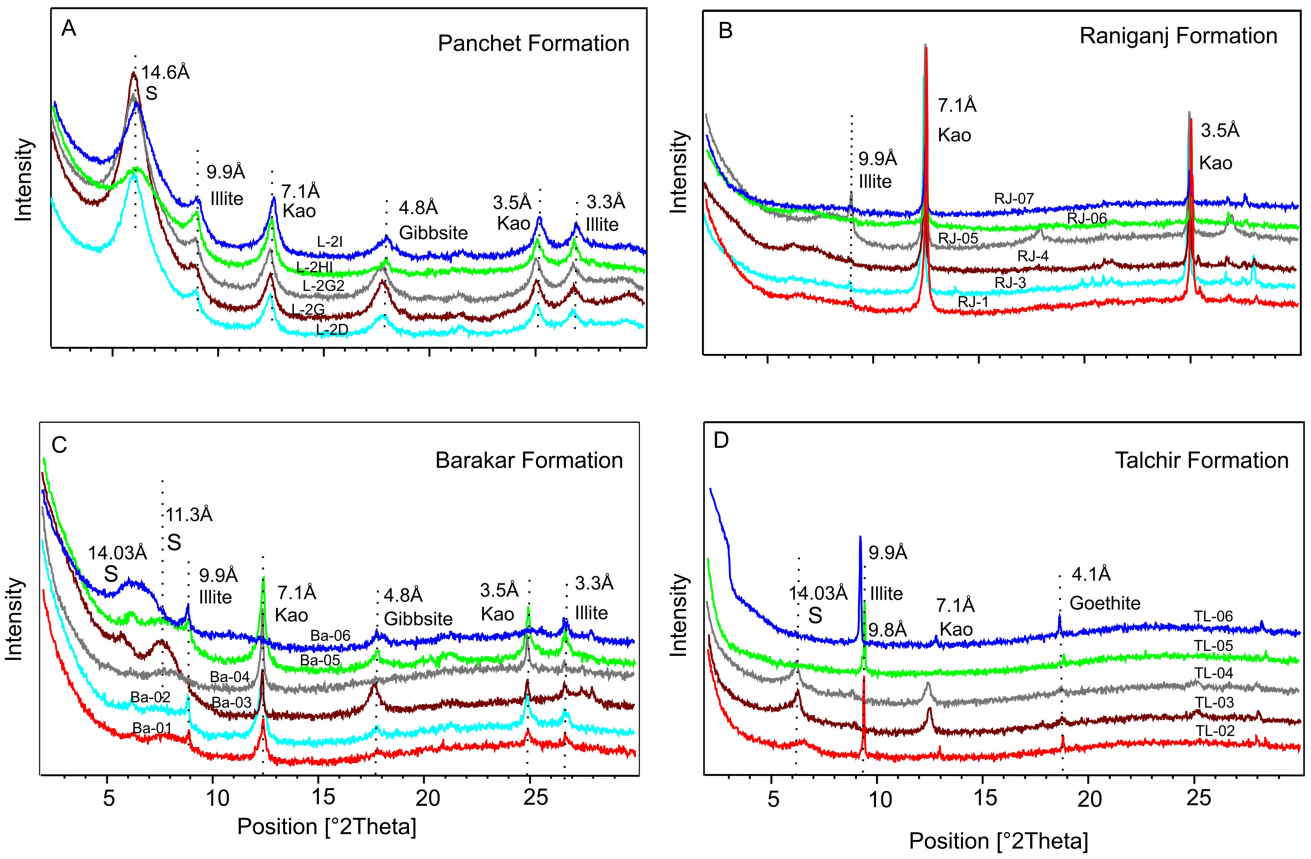

Fig. 3 XRD patterns of clay mineral fractions in different samples from different formations of the Raniganj Basin, in which diffraction intensity of the clay fractions are plotted with respect to 2θ values. Clay fractions, along with d-spacing in Å units, are labeled. S. smectite and kao-kaolinite, *I*. the peak area of the clay minerals used

3.3 Major and trace element analyses

The major and trace element concentration data [including rare earth elements (REEs)] were generated from siliciclastic sediment samples ($n = 35$) from the Raniganj Basin. Loss on ignition (LOI) was examined by heating 8 g of samples at 950 °C for 5 h. For geochemical analysis, 30 mg of homogenized powdered samples were digested with a mixture of $HF + HNO_3 + HClO_4$ acids in a closed Teflon® crucible (also see Xiong et al. 2012). Two United States Geological Survey (USGS) standard samples, Green River shale (SGR-1b) and Cody shale (SCO-1), were used as a calibration standard for the analysis. The concentration of major elements for the siliciclastic sediment samples from the Raniganj Basin was measured using inductively coupled plasma optical emission spectroscopy (ICP-OES; Agilent 5800 series). ICP-OES analysis used single-element solutions for the major elements (Ti, Al, Fe, K, Na, Ca, Mn, Mg, and P). The concentrations of trace elements (and REE) of each sample were measured using quadrupole inductively coupled plasma mass spectrometry (Q-ICP-MS; Agilent 7700 Series). The ICP-MS also measured multi-element solutions formed by mixed-element reference solutions of inorganic ventures (71A, 71B, and 71D). The ICP-MS and ICP-OES analysis had a precision of ≤ 5% and accuracy of ≤ 8%. All measurements were carried out at the analytical instrumentation facility of the Birbal Sahni Institute of Palaeosciences, Lucknow, India.

4 Results

4.1 Petrography

Sandstone samples from the Raniganj Basin are poorly sorted, and their thin sections exhibit detrital grains of quartz, K-feldspar, plagioclase laths, elongated micaceous minerals, and few lithic fragments (see Fig. 4). Monocrystalline quartz grains are more common than polycrystalline grains, and are sub-rounded to sub-angular in shapes except for a few elongated quartz minerals. Detrital quartz grains are also surrounded by a few overgrowth quartz grains. The quartz minerals show wavy extinction. The sandstones have cementing materials of calcite, neoblast quartz grains, iron oxides, and clay matrixes. Coarse to medium and angular feldspar are commonly present. Orthoclase, plagioclase, and microcline are the common feldspar minerals. Cross-hatch twinning of microclines and Carlsbad twinning of orthoclase are seen in the thin sections (see Fig. 4F). The plagioclase minerals show parallel twinning and are elongated in shape. Lithic fragments are mainly of sedimentary and igneous rocks.

4.2 Clay mineralogy

The clay fractions of the samples from different formations in the Raniganj Basin consist of smectite, illite, kaolinite, and traces of gibbsite and goethite (Fig. 3). Smectite (average value of ~ 79%), followed by illite (average value of ~ 8%) and kaolinite with an average fraction of ~ 14% are the main clay fractions in the Panchet Formation. Kaolinite becomes abundant in the Raniganj (~ 94%) and Barakar (~ 60%) formations, and illite content follows kaolinite in the Raniganj Formation (average fraction of ~ 5%) and Barakar Formation (~ 20%). The Talchir Formation has abundant clay content of illite (~ 65%) over smectite (~ 15%) and kaolinite (~ 20%). The relative content of clay fraction in the samples of different formations from the Raniganj Basin are listed in Supplementary material 3.

4.3 Major elements

The concentration of major elements (wt%) for studied samples from different formations of the Raniganj Basin are given in Supplementary material 4. The data show that SiO_2 concentration of the samples varies between 44.6 and 88.2 wt%. The Panchet and Barakar formations have wide ranges of silica concentrations. Samples of the Raniganj and the Talchir formations have higher values of silica content (> 70 wt%). The Raniganj Basin has a wide range of Al_2O_3 (5.04–20.9 wt%). The Raniganj Formation has depleted Al_2O_3 content, while the Talchir Formation shows an average value of Al_2O_3 content. The sample contents are low for CaO (0.55–3.5 wt%), MgO (0.58–3.06 wt%), and TiO_2 (0.07–1.12 wt%). Values of K_2O and Na_2O in the samples are 1.13–3.86 wt% and 1.25–4.41 wt%, respectively. There is wide range in values of SiO_2/Al_2O_3 ratios (2.13–17.46), but the average ratio is 5.06.

The values of weathering indices were measured based on the relative concentrations of mobile (Ca, Na, Mg, Mn and K) and immobile major (Al and Ti) cations of the rocks (Perri 2020) in different samples, including the chemical index of alteration (CIA, Nesbitt and Young 1982), chemical index of weathering that removes K-metasomatism effects (CIW, Harnois 1988), the plagioclase index of alteration (PIA, Fedo et al. 1995); the chemical index of weathering excluded CaO (CIX; Garzanti et al. 2014), and the weathering index of Parker (WIP, Parker 1970) (see Supplementary material 4). The CaO* values used in the calculation of different weathering indices refers to only those in silicate fractions of sediments. The values of CaO are accepted as CaO* if $CaO \leq Na_2O$, but the values of Na_2O were considered as CaO* when $CaO > Na_2O$ (Bock et al. 1998; Lin et al. 2019). The chemical index of quartz (CIQ, Guo et al. 2024), calculated based on the CIA and WIP, was also

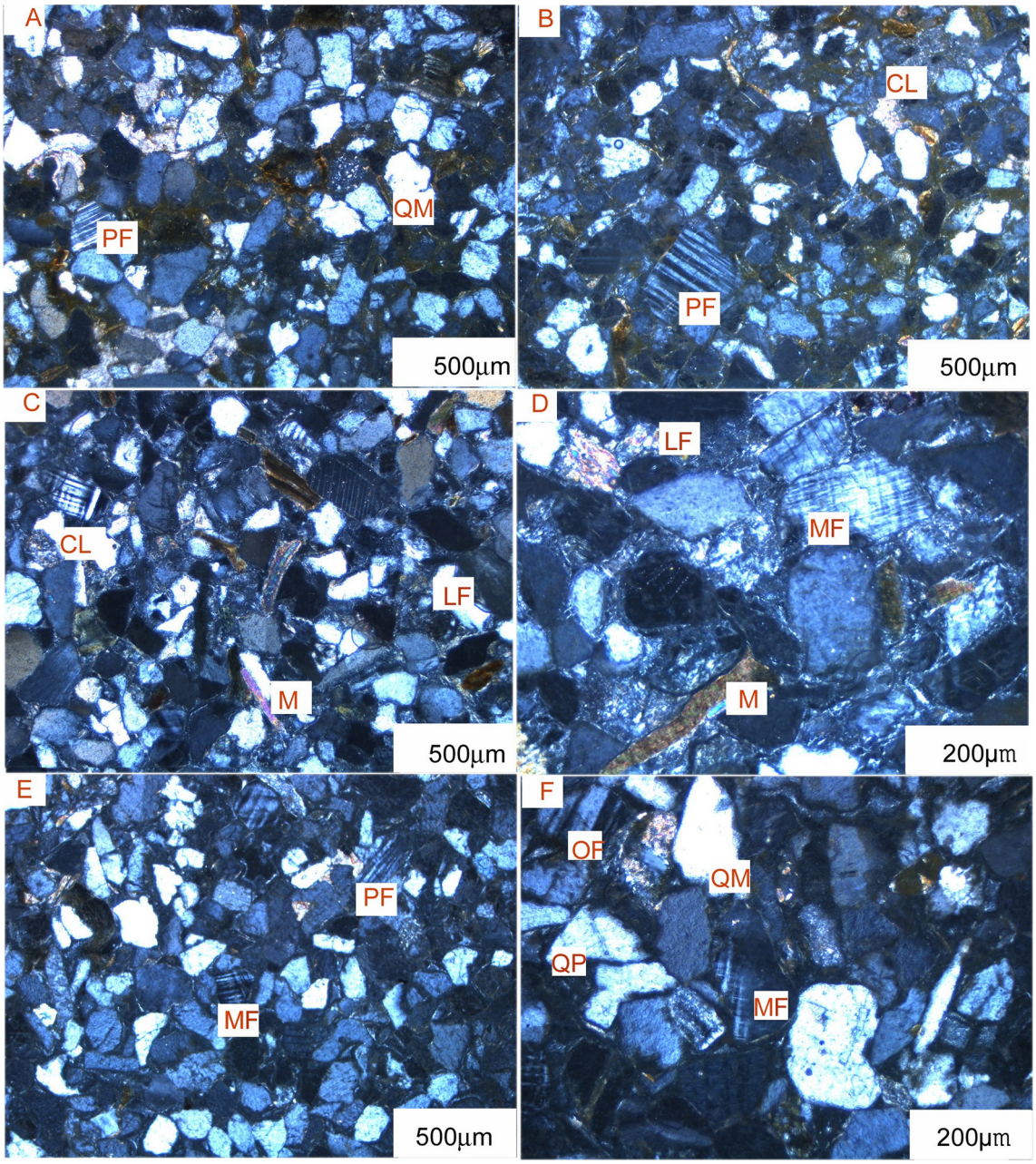

Fig. 4 Photomicrographs of the thin-section slide of the sandstone samples from Raniganj Basin. **A** Sub-rounded monocrystalline quartz grains (QM), and plagioclase (PF) in the sandstone slide. **B** Plagioclase grains (PF) and clay matrix (CL). **C** Clay matrix (CL) and mica grain (M). **D** Microcline feldspar (MF), lithic fragments (LF), and mica grain (M). **E** Microcline feldspar grain (MF) and plagioclase (PF). **F** Polycrystalline quartz grain (QP), monocrystalline quartz (QM), microcline (MF), and orthoclase feldspar (OF)

used to define quartz enrichment accurately. The Index of compositional variability (ICV), the relative abundance of other major cations over alumina, defined the sediment maturity (Cox et al. 1995). The correlation of Al_2O_3, Fe_2O_3, TiO_2, and MgO with SiO_2 was inversed (Fig. 5).

4.4 Trace elements

The trace element concentrations (ppm) (including REE) in the samples for different formations of the studied basin are shown in Supplementary material 5. The content of

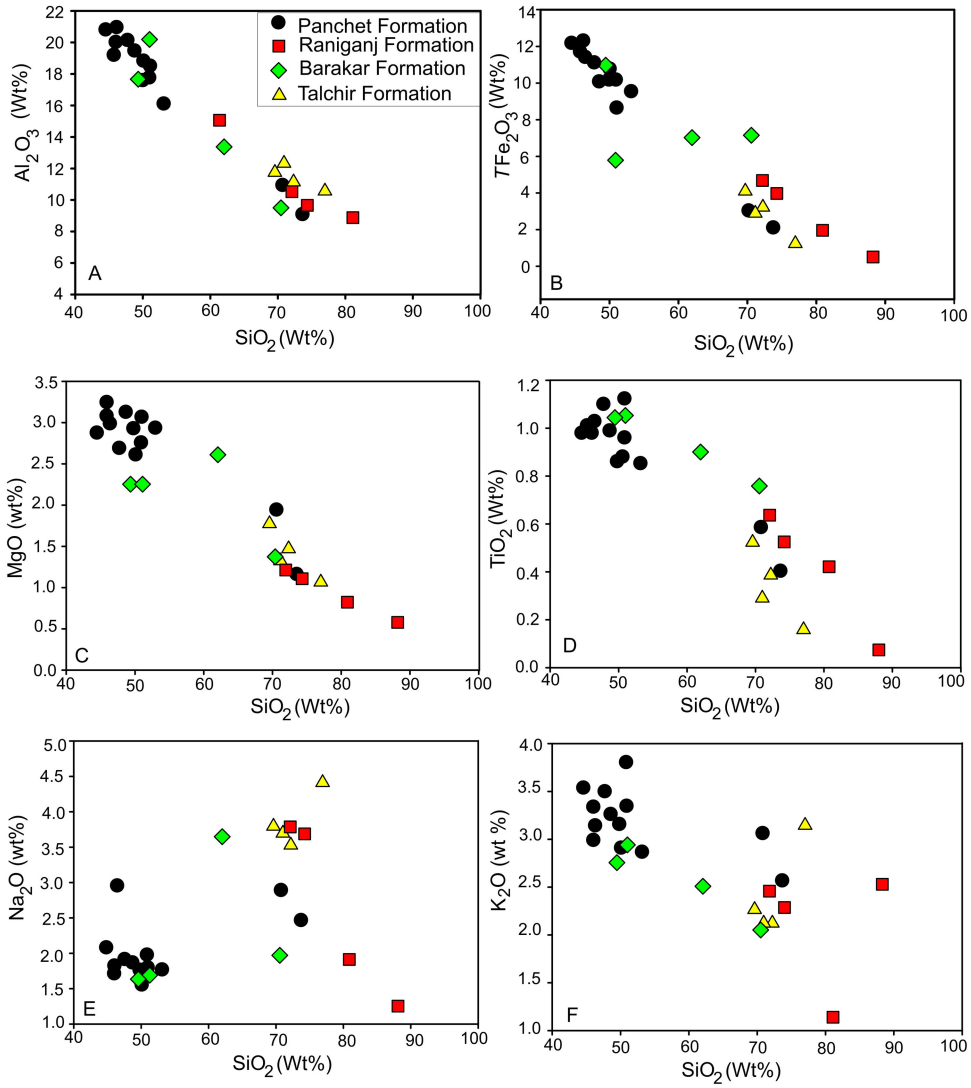

Fig. 5 Harker's variation diagrams for the different formations of the Raniganj Basin (after Harker 2011)

large-ion lithophile elements (LILEs) such as Rb, Pb, and Ba is comparatively equal to or greater than that in the upper continent crust (UCC) in the Panchet, Raniganj, Barakar, and Talchir formations. There are consistent values in the content of Pb. However, all the formations have low values of Sr content except for the Talchir Formation, having average Sr content (189 ppm) (Fig. 6). The values of Rb (average value = 156 ppm) and Ba (average value = 1295 ppm) in the Panchet Formation are relatively higher than that of other formations (Raniganj, Barakar, and Talchir formations).

The high-field-strength elements (HFSEs) like Th, Hf, and Nb have varied values, relative to the UCC values, but Y content is greater than or similar to the UCC values. Samples of the Panchet Formation have higher values of Hf (average value = 4 ppm) and Th (average value = 18 ppm) than the other formations. In samples of the Panchet Formation, values of transition metals such as Sc, V, Co, and Ni are comparatively similar to or greater than the UCC, while those of Raniganj and Talchir samples have values lower than or similar to the UCC. The values of Sc, V, Co, and Ni from the Barakar Formation samples are widely varied. Samples of the different formations from the Raniganj Basin show low values of Cr. The Panchet Formation has the highest Th/Sc ratio (average value = 1.08) compared to the rest of the formations. The Raniganj Formation has higher Co/Th ratios (average value = 2.85). The La/Sc ratio (average = 4.15) of Talchir Formation samples is highest compared with that of the other formations from the Raniganj Basin.

The REE concentrations of the studied samples and their parameters are given in Supplementary material 5. The UCC-normalized REE patterns of the samples are shown in Fig. 7. Siliciclastic sediment samples from the Raniganj Basin show no significant fractionation between the light rare earth elements (LREEs) and heavy rare earth elements (HREEs), as suggested by average values of $(La/Yb)_N = 1.29$ and $(\Sigma LREE/\Sigma HREE)_N = 0.87$ from the Raniganj Basin. Among the HREEs of the studied samples, there is depletion in Tb but enrichment in

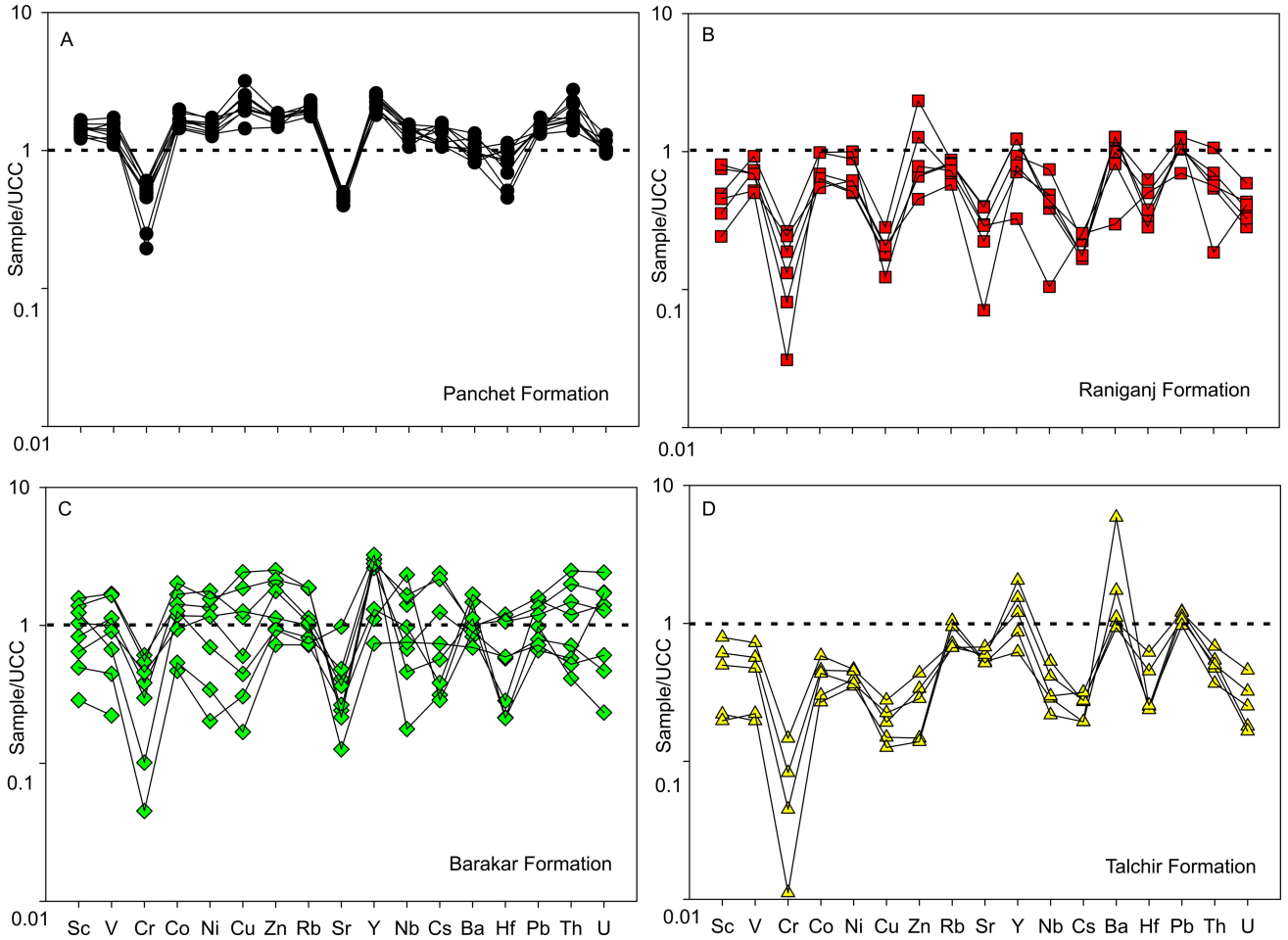

Fig. 6 Spider diagrams for the trace element compositions normalized against the average upper continental crust (UCC) values (Rudnick and Gao 2003) for the siliciclastic sediment samples of Panchet, Raniganj, Barakar, and Talchir formations

Gd and Tm (Fig). The samples have flat LREE patterns $(La/Sm)_N = 1.29$ (average) and flat HREE patterns $(Gd/Yb)_N$ = average 1.05. Some of the samples from the Raniganj Basin have lower concentration of REE compared to the UCC, particularly in samples from Raniganj and Talchir formations (Fig. 7). The Eu anomalies of the Raniganj Basin have commonly positive values (average values of Eu/Eu* = 1.45). In the samples of the Panchet Formation, the range in values for $(La/Sm)_N$, $(Gd/Yb)_N$, and Eu/Eu* are 1.02–1.26, 0.97–1.35, and 1.04–2.26, respectively. In the Raniganj Formation, the samples have values of $(La/Sm)_N = 0.79–1.25$, $(Gd/Yb)_N = 0.67–1.74$, and Eu/Eu* = 0.21–1.14. Barakar samples have the values of $(La/Sm)_N = 0.91–1.08$, $(Gd/Yb)_N = 0.67–1.74$, and Eu/Eu* = 0.73–2.44. The samples of the Talchir Formation have $(La/Sm)_N = 1.01–1.49$, $(Gd/Yb)_N = 0.47–1.17$, and Eu/Eu* = 1.02–1.73.

5 Discussions

5.1 Hydrodynamic sorting and sedimentary recycling effect

The source rock compositions, hydrodynamic sorting, and sedimentary recycling influence the chemical weathering and mineralogical and geochemical compositions of the sediments (Nesbitt and Young 1996; Garzanti et al. 2011; Guo et al. 2018, 2021, 2024). Hydrodynamic sorting commonly generates immature rock fragments or detrital minerals, inferring the quantity between the weathering product and unweathered source rock in the fluvial sediments (Guo et al. 2021, 2018, 2024). The CIQ vs. CIA/WIP diagram (Fig. 8; Guo et al. 2024) clearly indicates the effects of weathering intensity, hydrodynamic sorting, and sedimentary recycling on the sediment composition. Sediment samples of the Panchet Formation have low values of CIQ (ranges from 0.01 to

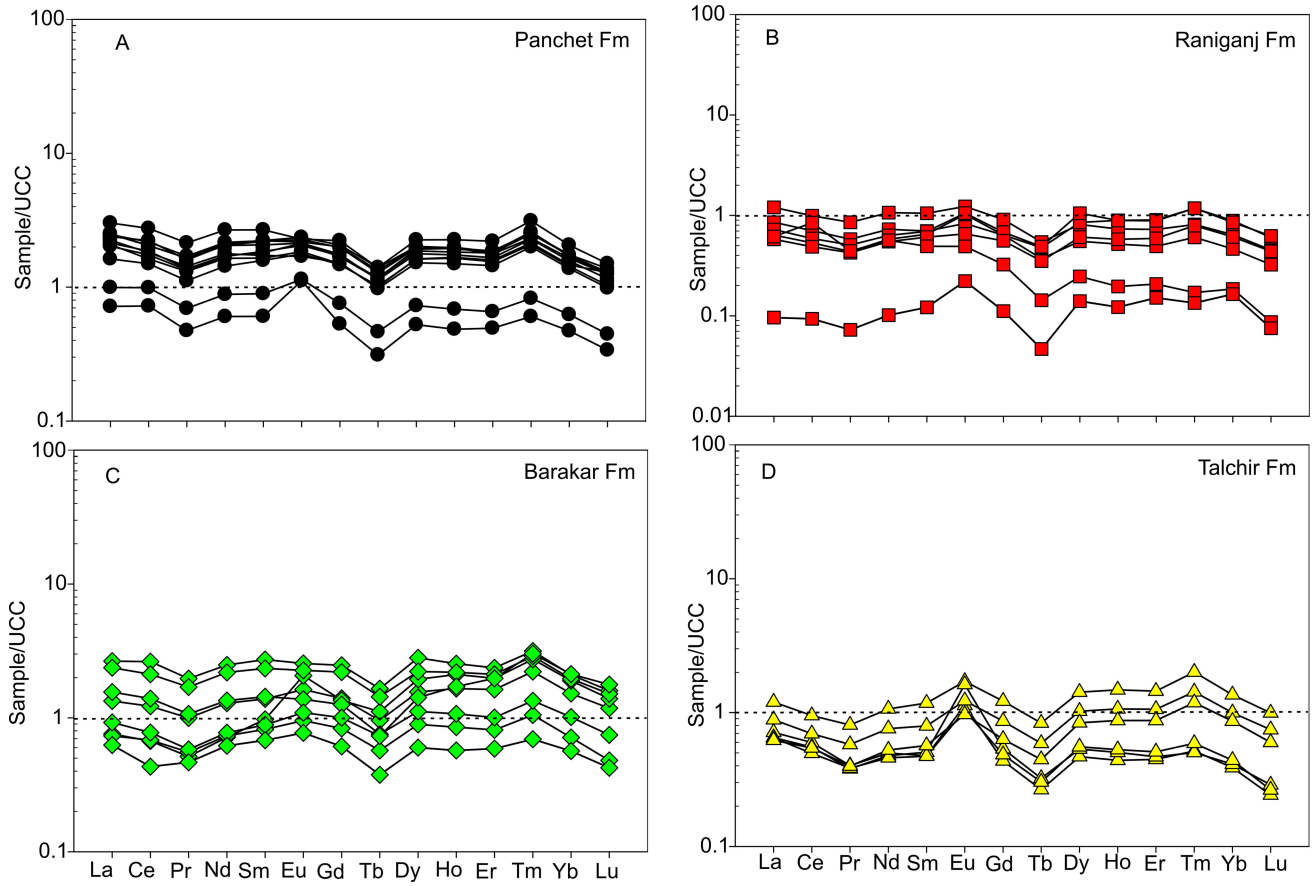

Fig. 7 UCC-normalized REE patterns for the samples of the Raniganj Basin. The UCC normalization values are from Rudnick and Gao (2003)

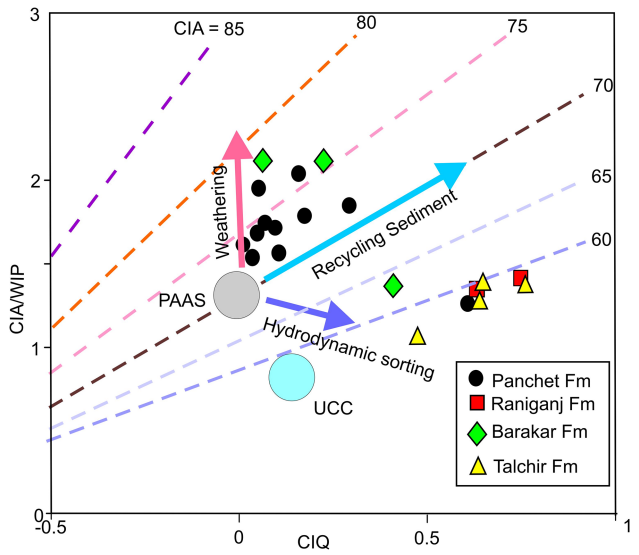

Fig. 8 CIQ vs. CIA/WIP diagram (after Guo et al. 2024) showing chemical weathering, recycling, and hydrodynamic sorting effects on the studied siliciclastic sediment samples from Raniganj Basin, along with the identified trends. The UCC and post-Archean Australian shale (PAAS) values are from Rudnick and Gao (2003) and Taylor and McLennan (1985), respectively

0.6), scattered values of CIA/WIP (1.2 to 2.04), and a positive correlation between CIQ and CIA/WIP (Fig. 8). This suggests a combination of both weathering and sedimentary recycling effects on the sedimentation of the Panchet Formation. The Raniganj Formation has sediment CIQ values (ranging from 0.6 to 1.8) and CIA/WIP values (widely ranging from 1.3 to 3.2) that have been influenced by both hydrodynamic sorting and sedimentary recycling. However, some of the samples from the Raniganj Formation are outliers to their trends in the CIQ vs. CIA/WIP diagram. The sediment samples of the Barakar Formation have a wide range of CIQ values (0.05 to 1.02) and CIA/WIP ratios (1.3 to 2.1). Therefore, compositions of some of the Barakar samples are influenced by chemical weathering, while some others are related to hydrodynamic sorting and sedimentary recycling processes (Fig. 8). The low CIA/WIP ratios (1.0 to 1.3), high CIQ values (0.4 to 0.7), and the slightly positive correlation between CIQ and CIA/WIP (Fig. 8) of the sediment samples from the Talchir Formation indicate that there were both hydrodynamic sorting and sedimentary recycling effects during the sedimentation in this particular formation.

The ratio between SiO_2 and Al_2O_3 also indicates the effects of hydrodynamic sorting and recycling sediments,

as the resistivity values of the quartz during the sedimentation are far higher than feldspar, lithic fragments, and mafic minerals (Bouchez et al. 2011; Guo et al. 2018, 2024). High values of Al_2O_3/SiO_2 ratios are related to the suspended load sediments (in low-energy flow), while low values of the ratio (angular quartz grain rich) suggest a bed load sediment (Guo et al. 2018). The average values of Al_2O_3/SiO_2 ratios for the samples from the Panchet and Barakar formations are 0.35 and 0.27, respectively, which are relatively higher than the average values for the Raniganj (0.11) and Panchet (0.15) formations. Therefore, the ratios also support the higher effects of hydrodynamic sorting and recycling sediments on the Talchir and Raniganj formations compared to the Barakar and Panchet formations. Cox et al. (1995) reported that mature sediments from the stable continental crust have low ICV values (< 1.0), while those of immature sediments of the arc-related volcanic and plutonic source rocks have higher ICV values (> 1.0). The average ICV values (> 1) for the Talchir, Barakar, Raniganj, and Panchet formations (Supplementary material 4) suggest compositionally immature sediments, possibly connected with the plutonic sources. The immature sediments of the Raniganj Basin inferred from the geochemical studies are also similarly suggested by the subangular- to angular-grained feldspar and quartz minerals of the sandstones from the Raniganj Basin (Fig. 4). Such immature sediments with angular grains of quartz and feldspar also suggest that the sediments were likely derived from a proximal source.

5.2 Diagenetic effect

The process of diagenesis may control the geochemical compositions of the sediments after the deposition (Hundert et al. 2006). In terrestrial depositions, water circulation in a thick succession of sedimentary rock induces diagenesis that accelerates the enrichment of some mobile elements (Nesbitt and Young 1989). It therefore makes uncertain the weathering and climatic signature of the source area. In the Raniganj Basin, the XRD analysis recorded no chlorite clay fraction from the samples (Supplementary material 3). Therefore, chloritization has no significant factor for the weathering and climatic interpretation of the Raniganj Basin. The abundant illite content in the Talchir Formation is possibly detrital clay minerals, as there is no evidence of illitization in CIA, CIW, and PIA values. Post-depositional K-metasomatism/illitization could change CIA values (Fedo et al. 1995; Wang et al. 2012). However, the values of CIA for the sediment samples from the Raniganj Basin are closer to that of CIW and PIA values than that calculated by removing K-metasomatism/illitization effects (Harnois 1988; Fedo et al. 1995), as shown in Supplementary material 4. It therefore indicates that the sedimentary rock samples of the studied area have no significant effect from the K-metasomatism/illitization.

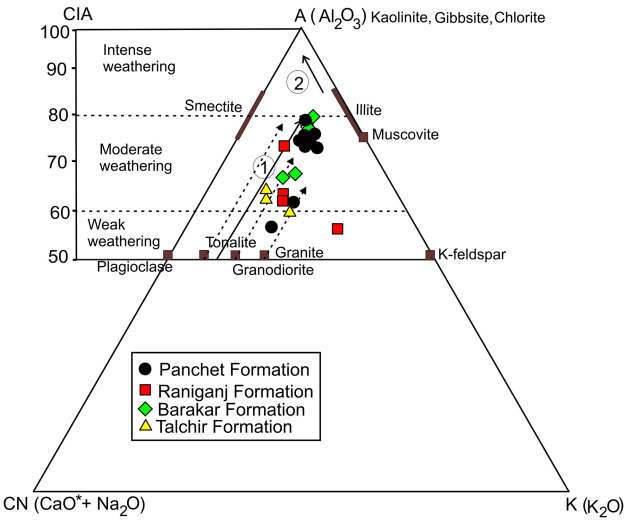

Fig. 9 Al_2O_3–CaO + Na_2O–K_2O diagram (after Nesbitt and Young 1984) for the siliciclastic sediment samples of the different formations of Raniganj Basin, India. The dashed lines suggest the ideal weathering trends for tonalite, granodiorite, and granite (Condie 1993). In the diagram, the number 1 represents the initial stage of chemical weathering, the number 2 represents the final stage of chemical weathering, and the dotted rays represent the trends of chemical weathering for the rock sources

Again, in the A-CN-K (Al_2O_3–CaO^* + Na_2O–K_2O) diagram as well (Fig. 9), the weathering trend is along the ideal weathering direction of granodiorite, not directed trend towards the K-apex, which therefore supports the insignificant post-depositional K-metasomatism/illitization conditions (Fedo et al. 1995; Wang et al. 2012).

Hydrodynamically sorted and immature sandstones are more common at the greater depth of the Talchir Formation compared to the upper depth of the Panchet Formation (see above discussion 5.1). The petrography of the sandstones from the Raniganj Basin (Fig. 4) also show commonly unaltered quartz, feldspar grains, simple grain contact, and no commonly pressure-solved and welded grains. Therefore, petrography and inference of immature sediments and/or detrital minerals from the geochemical characters also support a less chance of diagenetic influence on the sedimentary rocks of the Raniganj Basin. Previous studies also suggested that the basin itself had a small catchment area with a few rock types consequently characterized by clay fractions, related to syndepositional climatic changes (Suttner and Dutta 1986; Ghosh et al. 2019).

5.3 Chemical weathering and climatic changes

The weathering process significantly affects the chemical composition of sedimentary deposits (Nesbitt and Young 1982; Armstrong-Altrin et al. 2004). Different geochemical parameters are used to measure the weathering intensity of

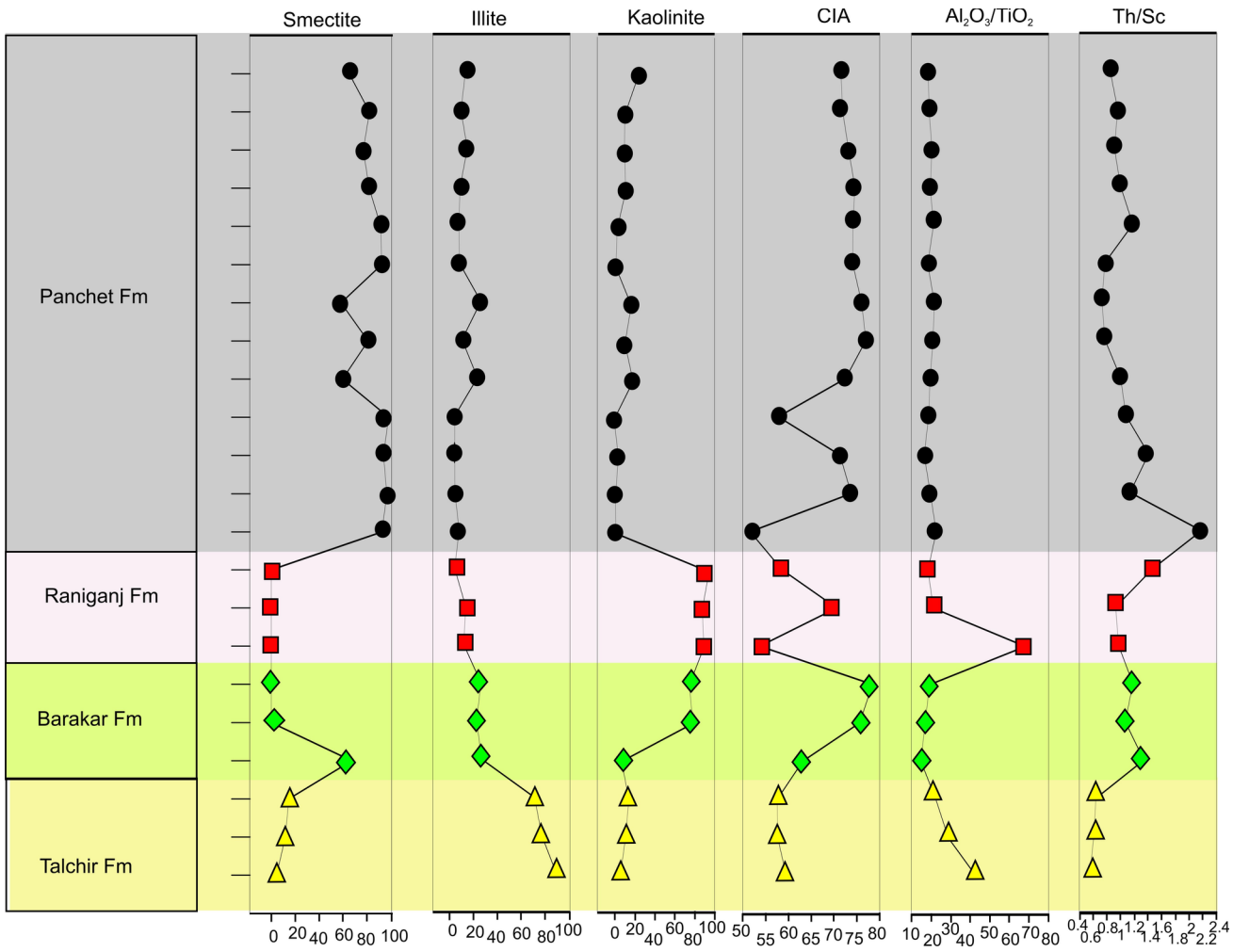

Fig. 10 Variations in CIA values with clay mineral content and a few elemental ratios (including major and trace elements) of the studied samples in the stratigraphic column of Raniganj Basin

the source rock. The CIA values define chemical weathering intensity as unweathered (CIA ≤ 50), incipient weathered (CIA = 50 to 60), intermediate (CIA = 60 to 80) and intense weathered (CIA > 80) (Nesbitt and Young 1982; Fedo et al. 1995). The stratigraphic variations (sampled profiles) of CIA along with clay fraction content and certain immobile major and trace element ratios are shown in Fig. 10. The siliciclastic sediment samples of the Talchir Formation of the Raniganj Basin have low CIA (55–59), which indicates low intensity of chemical weathering at the source area, while the values of CIA for the samples of the Barakar (CIA = 63–78), Raniganj (CIA = 53–70), and Panchet formations (CIA = 51–76) suggest moderate chemical weathering conditions at the source area. The similar weathering trends of the Raniganj Basin could also be suggested from the values of the CIW and PIA weathering indices, but these proxies have yielded only slightly higher values than the CIA values of the same samples (Supplementary 4).

Moreover, the CIA is usually used along with the A-CN-K (Al_2O_3–CaO* + Na_2O–K_2O) triangular diagram (Nesbitt and Young 1984; Fedo et al. 1995) to define weathering intensity. In the A-CN-K plot (Fig. 9), the Talchir samples cluster near initial weathering trends of the granodiorite, suggesting a weak weathering trend of felsic source rocks for the deposition of the Talchir Formation. In this plot, the Barakar and Panchet samples cluster within the moderate weathering trends, suggesting moderate weathering intensity. Sediments of the Raniganj Formation have experienced weak to moderate weathering conditions at the source area, as shown by scattered data points in the A-CN-K plot (Fig. 9).

Climatic conditions, mainly the temperature and precipitation, have influenced the chemical weathering intensity of the source rocks, as cold/temperate climate induces a low chemical weathering trend of bedrock, while humid and warm climate relates to intense chemical weathering

conditions (e.g., Nesbitt and Young 1982; Perri 2020; Wang et al. 2020). Previous clay mineral studies have recorded that chemical weathering of bedrock under semi-arid climatic conditions could produce clay minerals such as illite/smectite mixed clay and smectite minerals (Thiry 2000; Adatte et al. 2002; Sheldon and Tabor 2009), whereas intense weathering of bedrock under warm and humid climate could produce kaolinite and gibbsite (Hieronymus et al. 2001; Beckmann et al. 2005; Ratcliffe et al. 2010). The abundant clay content of illite over the kaolinite, and smectite in the siliciclastic samples of the Talchir Formation are consistent with a physical weathering condition during cold/arid climate conditions. Also, the smectite abundance over the kaolinite and illite clay content of the Panchet Formation suggested a semi-arid climate during the deposition of these sediments. The relatively higher values of Rb and Al_2O_3 in the Panchet Formation indicate that the Rb may relate to the clay contained in the studied samples of the formation (see Supplementary material 4 and 5) (Hu et al. 2015; Wang et al. 2017). However, the dominant kaolinite clay content in the Barakar and Raniganj formations could suggest a humid and warm climate and also be a result from the recycled sediments that survive during intermediate weathering conditions (Weaver 1967). The CIQ vs. CIA/WIP ratio variation plot, as discussed above, also suggested that sediments of the Barakar and Raniganj formations have a recycled sediments source.

Thus, in summary, the weathering indices and clay mineralogy suggest that the climatic conditions of the Raniganj Basin could possibly have cold, arid conditions for the Talchir Formation, contrasting with the Barakar, Raniganj, and Panchet formations which had a fluctuation in climate from semi-arid condition to slightly humid during their sedimentation.

5.4 Provenance

The elemental concentrations in the sedimentary rock provide clues for the provenance study of a basin (Verma and Armstrong-Altrin 2013, 2016; Armstrong-Altrin et al. 2015, 2017; Wang et al. 2018; Wanas and Assal 2021, Sangeeta et al. 2023). The Al_2O_3/TiO_2 ratios of the studied samples could infer their provenance, as previous studies indicate that the ratios have ranges of 3–8, 8–21, and 21–70 for mafic, intermediate, and igneous source rocks, respectively (Hayashi et al. 1997; Moradi et al. 2016; Wang et al. 2017, Wang et al. 2018). Therefore, the Al_2O_3/TiO_2 ratio (12.56–28.82; average = 19.43) of the studied samples suggests an intermediate igneous rock source (Supplementary material 4).

Moreover, the trace elements (REE, Th, Y, Nb, Hf, Sc, Co, Cr, and Ni) remain stable in the sediments during the weathering and transportation and, therefore, are used to interpret the source rock of the sediment samples (Taylor and McLennan 1985; Bhatia and Crook 1986; Cullers and Berendsen 1998; Fedo et al. 1995; Mongelli et al. 2006; Wani and Mondal 2011; Moradi et al. 2016; Song et al. 2017). Felsic rock contains a relatively high concentration of La and Th, whereas mafic rocks generally show relatively high concentrations of Co, Sc, Cr, and Ni (Cullers 1994, 2000; McLennan 1993). It is also known that elemental ratios such as La/Sc, Th/Sc, and Cr/Th are commonly used to differentiate the felsic source from the mafic one (Armstrong-Altrin et al. 2004, 2013; Bhatia 1983; Hayashi et al. 1997; Cullers and Podkovyrov 2000; Sindhuja et al. 2021). Thus, the elemental ratios of the above trace elements are also applied in our present study.

The UCC-normalized REE patterns (Fig. 7) of the studied samples show the enrichment of Gd and Tm within the HREE. The enrichment could be related to the HREE-enriched heavy minerals such as zircon and garnet (Sawant et al. 2017; Wang et al. 2018) as the Talchir samples show positive correlation ($R = 0.91$) between Tm and Hf elements. The heavy mineral content in the sediment samples of the Raniganj, Barakar, and particularly the Talchir formations have also been supported by the CIQ vs. CIA/WIP diagram (Fig. 8), illustrating the effect of hydrodynamic sorting and sedimentary recycling processes on the sediment samples. However, the significant correlation ($R = 0.87$) between LREE and HREE of the sediment samples suggest that the REE content is distinctively controlled by a single factor, possibly the source rock (Wang et al. 2018). There is also no distinct fractionation between the LREE and HREE of the studied samples, as given by the average values of $(La/Yb)_N$, $(Gd/Yb)_N$, and $(\Sigma LREE/\Sigma HREE)_N$ (Supplementary material 5). Thus, it could be concluded that though there is evidence of heavy mineral content in the studied samples, the influence of heavy minerals on the REE content of the sediments in the basin is not significant.

Felsic rock has a high negative Eu anomaly, but mafic rock shows a gentle or no Eu anomaly (Roddaz et al. 2006; Armstrong-Altrin et al. 2017; Moradi et al. 2016; Wang et al. 2017). Granulite facies of felsic rock protoliths that represent the residue after partial melting usually possess positive Eu/Eu* values (McLennan and Taylor 2011). Therefore, the significant positive Eu anomalies (average 1.45) for the studied samples of the Raniganj Basin could be related to sediment sources from the granulite facies of felsic rock protoliths such as charnockite, an intermediate rock of granulite facies that is one of the main rocks of the CGGC, the basement of the Raniganj Basin (Acharyya 2003). The high values of Y in a few samples of the Talchir and Barakar formations (Fig. 6), relative to the UCC, are due to content of mineral sphene in the sediments (Ghosh and Sarkar 2010). In the Sc vs. Th/Sc diagram (Fig. 11), the studied clastic sediments are

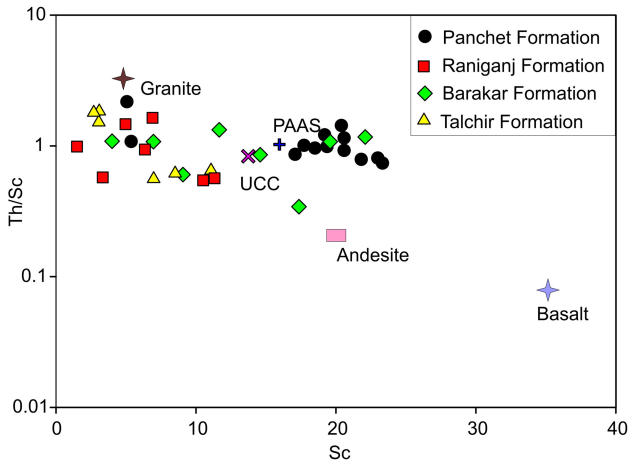

Fig. 11 Th/Sc versus Sc bivariate plot for siliciclastic sediments (Nagaranjan et al. 2017), PAAS, UCC (Taylor and McLennan 1985; McLennan 2001), granite, andesite, and basalt (Condie 1993)

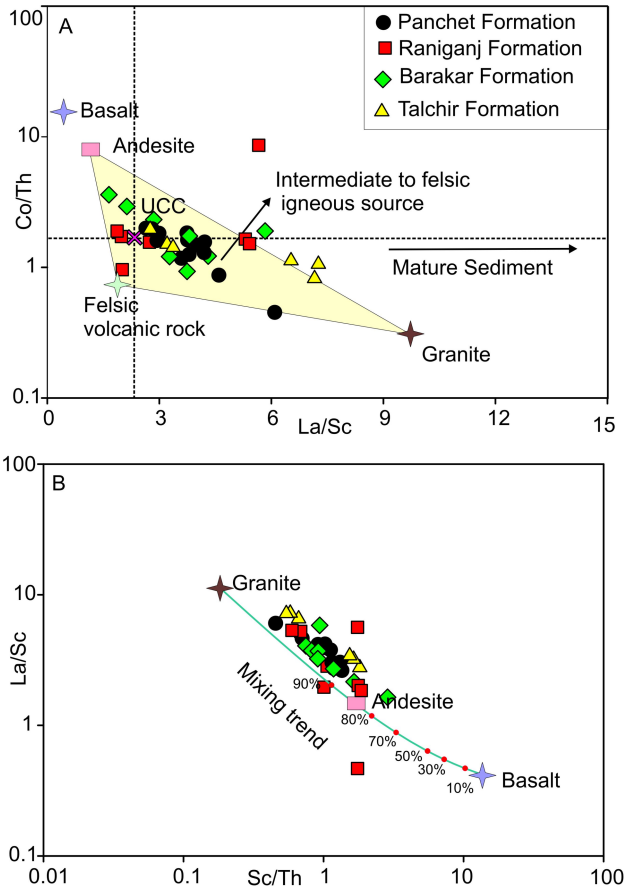

Fig. 12 A La/Sc vs. Co/Th diagram (after Gu et al. 2002); average composition of igneous rocks are from Condie (1993) and UCC (after Taylor and McLennan 1985; McLennan 2001). B Sc/Th vs. La/Sc diagram of the different formations of Raniganj Basin showing the mixing trend of granite and basalt end members from the Chotangpur granite gneissic complex (CGGC), the basement of the Raniganj Basin. Data source: granite, basalt, and andesite of CGGC after Ashima et al. (2014). UCC. upper continental crust

plotted towards the field of the intermediate to felsic source rocks, indicating the intermediate to felsic source of these sediments. The felsic to andesitic composition for the sediment samples of the Raniganj Basin is also evidenced from the La/Sc vs. Co/Th diagram (Fig. 12A). A similar source character in the sedimentation is again assured by the low values of Cr/Th ratio (0.2–3.78), as sediments originating from a felsic source have low Cr/Th ratios ranging from 0 to 15, whilst those of a mafic source have higher rations ranging from 22 to 500 (Cullers 2000; Roddaz et al. 2005, 2007). In the La/Sc–Sc/Th diagram (Fig. 12B), along with the available data of granite, andesite, and basalt from the basement rocks (CGGC; Saikia et al. 2014), our samples are trending close to the mixing trend of granite and basalt end members from the CGGC, plotted near the granite end member and away from the mafic end member. Thus, the source of our study sediments could be felsic to andesitic rock and possibly derived from the basement rocks (CGGC). The recycled sediments could also possibly relate to the metasediment components of the CGGC (Acharyya 2003).

The possible provenance for the sediments of the Raniganj Basin could be the CGGC, the Singhbhum folded belt, or the Archaean Singbhum Craton based on the geological setting, paleocurrent direction, and chemical composition of sediments in the basin. Pascoe (1956) and Dutta (1983) also reported that the Raniganj Basin sediments mostly came from the adjoining Precambrian basement CGGC. It was also recorded that the ages of apatites with fission track dating from the Raniganj and Panchet formations showed that the basin sediments were possibly transported from the CGGC (Patel et al. 2014). However, the provenance of the Raniganj Basin could have a lower chance of being from the Archaean Singbhum Craton and Singbhum Folded Belt for the following reasons: (1) the dominant rocks of the Singbhum Folded Belt of Proterozoic age are meta-sediments and metabasic rocks (Saha 1994; Sengupta et al. 2000; Mazumder et al. 2012), which is very different from the dominant felsic to the intermediate source of the Raniganj Basin sediments; (2) the Raniganj basin itself is within the extensive CGGC terrain; and (3) the common paleocurrent direction of the sedimentation is from the east–southeast to west–northwest direction (Casshyap and Kumar 1987). Thus, the only possible source could be the CGGC, constituted by porphyritic granitoid and charnockites (pyroxene-bearing granitoids) with enclaves of mafic granulites, khondalites (i.e., garnet-sillimanite gneiss), calc-silicates, and minor quartzite (Acharyya 2003).

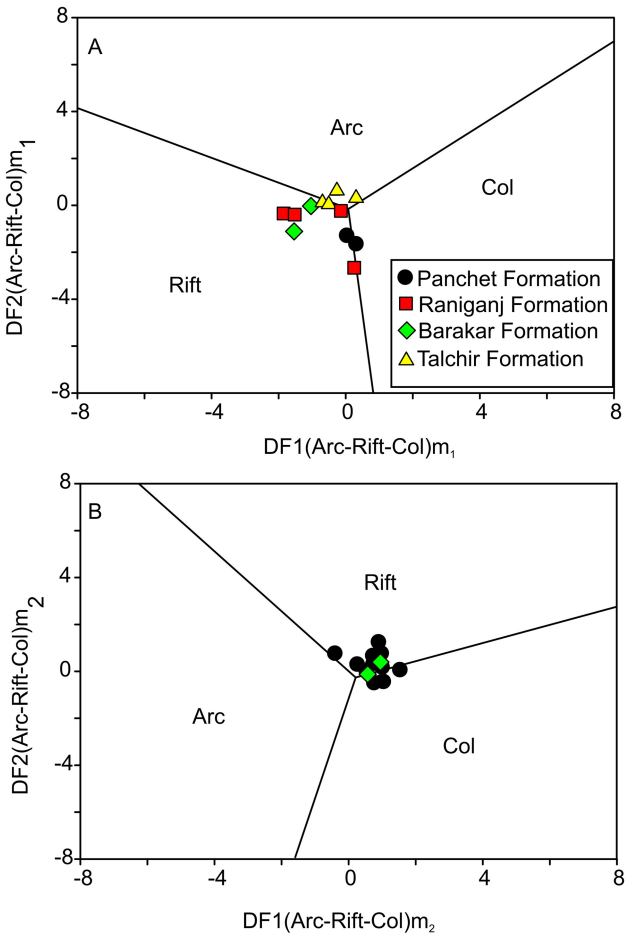

Fig. 13 Tectonic setting diagrams for the Raniganj Basin. **A.** Discriminant-function diagram for high-silica siliciclastic sediments. The subscript m_1 in DF1 (discriminant function 1) and DF2 (discriminant function 2) denotes the high-silica diagram based on $\log_e$-ratios of major elements. **B.** Discriminant-function diagram for low-silica siliciclastic sediments. The subscript m_2 in DF1 and DF2 denotes the low-silica diagram based on the $\log_e$-ratios of major elements. Both diagrams **A** and **B** after Verma and Armstrong-Altrin 2013

5.5 Tectonic evolution of the Raniganj Basin

The major and trace element abundances of siliciclastic sediments are helpful in differentiating the source tectonic settings for a sedimentary basin (Bhatia and Crook 1986; Roser and Korsch 1986; Verma and Armstrong-Altrin 2013; Taheri et al. 2018; Absar 2021). Verma and Armstrong-Altrin (2013) introduced two discriminant diagrams based on major elements of the siliciclastic sediments for discriminating the three main tectonic settings, such as island arc or continental arc, collision, and rift settings. The two discriminant diagrams (Verma and Armstrong-Altrin 2013) of the studied siliciclastic sediments suggest rift origin (passive) tectonic settings for the Raniganj Basin (Fig. 13). The diagrams also indicate that some sediments of the Raniganj Basin are associated with collision tectonic settings. The inferred rift tectonic settings (passive margin) of the Raniganj Basin are supported by the low Th/Sc values (0.59–3.04), as the low Th/Sc (< 3) indicates the depletion of plagioclase and unstable minerals in the passive margin setting (Bhatia and Crook 1986). The tectonic setting inferred by the geochemical studies is comparable to the regional geology of the Raniganj Basin. The rift tectonic setting of the Raniganj Basin, therefore, supports the idea of a pull-apart basin in the Damodar Valley, formed due to reactivation of the deeply buried lineaments/discontinuities of Precambrian time (see Naqvi et al. 1974; Kaila 1986; Mitra 1994; Acharyya 2000 and Chakraborty et al. 2003). The affinity of the collision tectonic setting in some samples of the Panchet and Raniganj formations (Fig. 13) could suggest the basement source signature without less alteration, as the basin itself forms within the CGGC, a part of the Central Indian Tectonic Zone (CITZ), which indicates a continent–continent collision event of major Indian blocks during Paleo-Neoproterozoic time (e.g., Acharyya 2003; Bhowmik et al. 2012).

Therefore, the basement CGGC contributed the source sediments throughout the basin formation of the Raniganj Basin, while there was shifting in the prevailing climatic conditions from the cool Talchir Formation to the semi-arid Barakar, Raniganj, and Panchet formations (Fig. 14). The abundant sediment sources of the basin were the felsic to andesitic rocks from the CGGC (Fig. 12B). The sedimentation of the Raniganj Basin took place on a rift basin, formed by reactivation of a primitive lineament (Fig. 13). A few samples from the Panchet and Raniganj formations suggested the affinity of collision setting. However, this study proves that the collision signature could have resulted from the Paleo-Neoproterozoic collision event in the CITZ.

6 Conclusions

The current study contributes new ideas towards an understanding of the paleo-weathering, paleoclimate, paleoenvironment, sources of deposited sediment, and tectonic features during the depositions of the sediments in the Raniganj Basin. Based on the study of mineralogical and geochemical studies of the Raniganj Basin, the main conclusions are given below:

1. The weathering and paleoclimatic studies of the studied samples suggests that in the Raniganj Basin, the Talchir Formation indicates low chemical weathering during cold/temperate climates, whilst that of the Barakar, Raniganj, and Panchet formations shows moderate weathering of semi-arid climatic conditions.

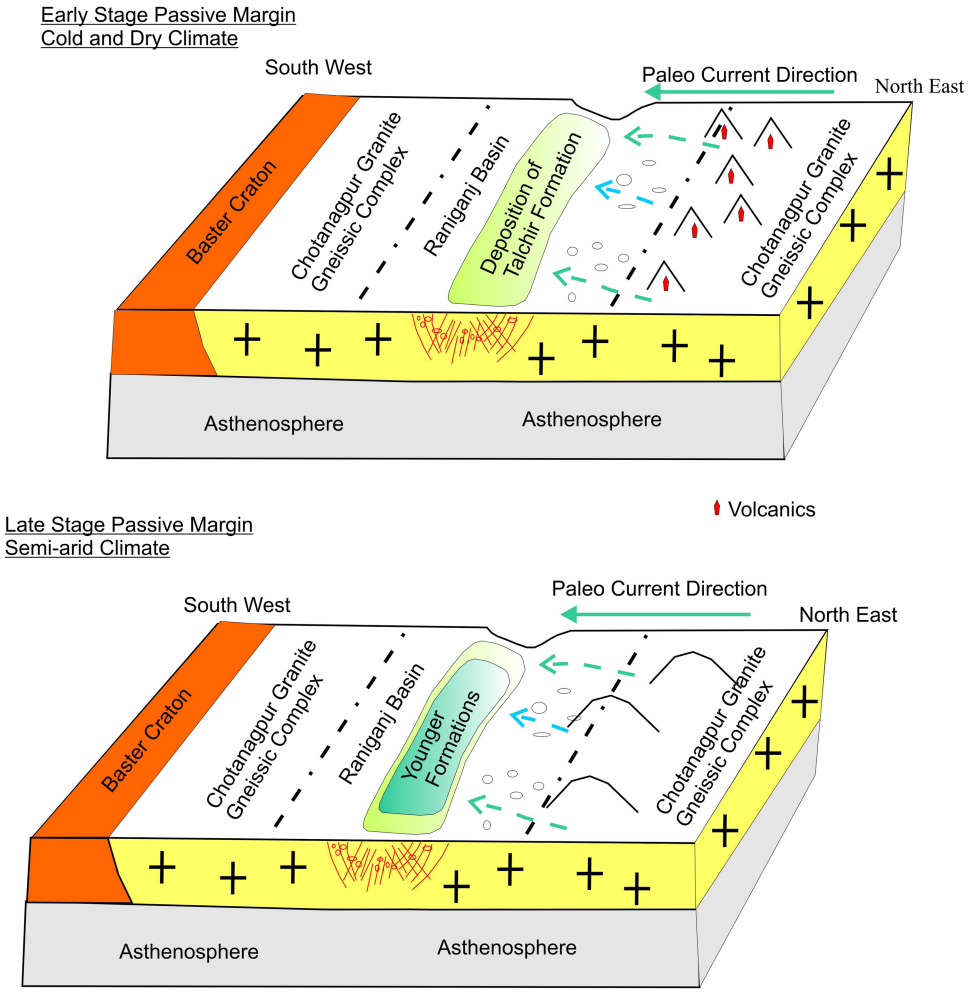

Fig. 14 Cartoon diagram depicting the evolution of the Raniganj Basin

2. The trace element concentrations of studied sediment samples from the Raniganj Basin, such as REE patterns, elemental ratios like La/Sc, Cr/Th, and Co/Th, and discrimination plots such as Hf vs. La/Th, Sc vs. Th/Sc, and La/Sc–Sc/Th diagrams, suggest that the provenance of the sediments might be from the CGGC which consists of porphyritic granitoid and charnockites with enclaves of mafic granulites, khondalites, calc-silicates, and minor quartzite.
3. The two tectonic setting discriminant diagrams based on major elements and low Th/Sc values in the studied siliciclastic sediments suggest a rift origin (passive) tectonic setting for the Raniganj Basin. The diagrams also indicate that some sediment samples of the Raniganj Basin are associated with collision tectonic settings. The affinity of the collision tectonic setting in some samples of the Panchet and Raniganj formations may be due to the basement CGGC source signature, formed by the collision of major Indian blocks, during Paleo-Neoproterozoic time.

Acknowledgements KM Sharma is thankful to SERB-DST for Early Career Research (ECR/2016/001100) and SERB CRG sanctioned no. CRG/2021/004627), and YPS is thankful to SERB for providing JRF. KM Sharma is also thankful to UGC for the start-up grant from UGC, No. F.30-4/ 2014 (BSR). OK is supported by an IoE Seed Grant (Dev. Scheme No. 6031) provided by Banaras Hindu University, Varanasi, India.

Authors' contributions KMS, RPT, and RP conceptualized the project. KMS, YPS, NPS, and NAS conducted geological field work and collected the samples. YPS and JKP prepared the geochemical and clay mineralogical samples. PK and Prem K conducted XRD analysis for clay mineral samples. AS conducted the geochemical analysis. OK, HT, and PG edited and reviewed the manuscript. All the authors contributed in writing this manuscript.

Funding K. M. Sharma was funded by SERB-DST, New Delhi, India for Early Career Research (ECR/2016/001100) during 2017 to 2021.

Data availability Not applicable.

Code availability Not applicable.

Declarations

Competing interests The authors affirm that they have no known competing financial interests or personal relationships that could influence the work presented in this paper.

Ethics approval Not applicable.

Consent to participate All authors listed in this manuscript agree to publication.

References

Abdulfarraj MR, Alqahtani FA, Wanas HA (2024) Petrography and geochemistry of sandstones of the ash shumaysi formation in the Jeddah-Makkah region, Saudi Arabia: implications for provenance, tectonic setting, paleoweathering, paleoclimate and paleogeography. Sediment Geol 460:106549

Absar N (2021) Mineralogy and geochemistry of siliciclastic Miocene Cuddalore Formation, Cauvery Basin, South India: Implications for provenance and paleoclimate. J Palaeogeogr 10(4):602–630

Acharyya SK (2000) Break up of Australia-India-Madagascar block, opening of the Indian Ocean and continental accretion in Southeast Asia with special reference to the characteristics of the peri-Indian collision zones. Gondwana Res 3(4):425–443

Acharyya SK (2003) The nature of Mesoproterozoic Central Indian Tectonic Zone with exhumed and reworked older granulites. Gondwana Res 6(2):197–214

Adatte T, Keller G, Stinnesbeck W (2002) Late Cretaceous to early Paleocene climate and sea-level fluctuations: the Tunisian record. Palaeogeogr Palaeoclimatol Palaeoecol 178(3–4):165–196

Algeo TJ, Kuwahara K, Sano H, Bates S, Lyons T, Elswick E, Maynard JB (2011) Spatial variation in sediment fluxes, redox conditions, and productivity in the Permian-Triassic Panthalassic Ocean. Palaeogeogr Palaeoclimatol Palaeoecol 308(1–2):65–83

Algeo TJ, Chen ZQ, Bottjer DJ (2015) Global review of the Permian-Triassic mass extinction and subsequent recovery: Part II. Earth Sci Rev 149:1–4

Armstrong-Altrin JS, Lee YI, Verma SP, Ramasamy S (2004) Geochemistry of sandstones from the Upper Miocene Kudankulam Formation, southern India: implications for provenance, weathering, and tectonic setting. J Sediment Res 74(2):285–297

Armstrong-Altrin JS, Nagarajan R, Madhavaraju J, Rosalez-Hoz L, Lee YI, Balaram V, Avila-Ramírez G (2013) Geochemistry of the Jurassic and Upper Cretaceous shales from the Molango Region, Hidalgo, eastern Mexico: Implications for source-area weathering, provenance, and tectonic setting. C R Geosci 345(4):185–202

Armstrong-Altrin JS, Nagarajan R, Balaram V, Natalhy-Pineda O (2015) Petrography and geochemistry of sands from the Chachalacas and Veracruz beach areas, western Gulf of Mexico, Mexico: constraints on provenance and tectonic setting. J South Am Earth Sci 64:199–216

Armstrong-Altrin JS, Lee YI, Kasper-Zubillaga JJ, Trejo-Ramírez E (2017) Mineralogy and geochemistry of sands along the Manzanillo and El Carrizal beach areas, southern Mexico: implications for palaeoweathering, provenance and tectonic setting. Geol J 52(4):559–582

Armstrong-Altrin JS, Botello AV, Villanueva SF, Soto LA (2019) Geochemistry of surface sediments from the north-western Gulf of Mexico: implications for provenance and heavy metal contamination. Geol Quart 63(3):522–538. https://doi.org/10.7306/gq.1484

Ashima S, Bibhuti G, Mansoor A, Talat A (2014) Geochemical constraints on the evolution of mafic and felsic rocks in the Bathani volcanic and volcanosedimentary sequence of Chotanagpur Granite Gneiss Complex. J Earth Syst Sci 123(5):959–987

Banerjee I (1966) Turbidites in a glacial sequence: a study from the Talchir Formation, Raniganj Coalfield, India. J Geol 74(5 Part 1):593–606

Beckmann B, Flögel S, Hofmann P, Schulz M, Wagner T (2005) Orbital forcing of Cretaceous river discharge in tropical Africa and ocean response. Nature 437:241–244

Bhatia MR (1983) Plate tectonics and geochemical composition of sandstones. J Geol 91(6):611–627

Bhatia MR, Crook KA (1986) Trace element characteristics of graywackes and tectonic setting discrimination of sedimentary basins. Contrib Mineral Pet 92(2):181–193

Bhattacharjee J, Ghosh KK, Bhattacharya B (2018) Petrography and geochemistry of sandstone–mudstone from Barakar Formation (early Permian), Raniganj Basin, India: implications for provenance, weathering and marine depositional conditions during Lower Gondwana sedimentation. Geol J 53(3):1102–1122

Bhowmik SK, Wilde SA, Bhandari A, Pal T, Pant NC (2012) Growth of the Greater Indian Landmass and its assembly in Rodinia: geochronological evidence from the Central Indian Tectonic Zone. Gondwana Res 22(1):54–72

Bock B, Mclennan SM, Hanson GN (1998) Geochemistry and provenance of the Middle Ordovician Austin Glen Member (Normanskill Formation) and the Taconian Orogeny in New England. Sedimentology 45:635–655

Bouchez J, Gaillardet J, France-Lanord C, Maurice L, Dutra-Maia P (2011) Grain size control of river suspended sediment geochemistry: clues from Amazon River depth profiles. Geochem Geophys Geosyst. https://doi.org/10.1029/2010GC003380

Casshyap SM (1979) Palaeocurrents and basin framework—an example from Jharia Coalfield, Bihar (India). In: Laskar B, Raja-Rao CS (eds) Fourth International Gondwana Symposium. Hindustan Publishing Corporation, Delhi, pp 626–641

Casshyap SM, Kumar A (1987) Fluvial architecture of the Upper Permian Raniganj coal measure in the Damodar basin Eastern India. Sediment Geol 51(3–4):181–213

Chakraborty C, Mandal N, Ghosh SK (2003) Kinematics of the Gondwana basins of peninsular India. Tectonophysics 377(3–4):299–324

Chatterjee N, Crowley JL, Ghose NC (2008) Geochronology of the 1.55 Ga Bengal anorthosite and Grenvillian metamorphism in the Chotanagpur gneissic complex, eastern India. Precambrian Res 161(3–4):303–316

Chen ZQ, Algeo TJ, Bottjer DJ (2014) Global review of the Permian-Triassic mass extinction and subsequent recovery: Part I. Earth-Sci Rev 137:1–5

Condie KC (1993) Chemical composition and evolution of the upper continental crust: contrasting results from surface samples and shales. Chem Geol 104(1–4):1–37

Cox R, Lowe DR, Cullers RL (1995) The influence of sediment recycling and basement composition on evolution of mudrock chemistry in the southwestern United States. Geochim Cosmochim Acta 59(14):2919–2940

Cui Y, Bercovici A, Yu J, Kump LR, Freeman KH, Su S, Vajda V (2017) Carbon cycle perturbation expressed in terrestrial Permian-Triassic boundary sections in South China. Glob Planet Change 148:272–285

Cullers RL (1994) The controls on the major and trace element variation of shales, siltstones, and sandstones of Pennsylvanian-Permian age from uplifted continental blocks in Colorado to platform sediment in Kansas, USA. Geochim Cosmochim Acta 58(22):4955–4972

Cullers RL (2000) The geochemistry of shales, siltstones and sandstones of Pennsylvanian-Permian age, Colorado, USA: implications for provenance and metamorphic studies. Lithos 51(3):181–203

Cullers RL, Berendsen P (1998) The provenance and chemical variation of sandstones associated with the Mid-continent Rift System, USA. Eur J Min 10(5):987–1002

Cullers RL, Podkovyrov VN (2000) Geochemistry of the Mesoproterozoic Lakhanda shales in southeastern Yakutia, Russia: implications for mineralogical and provenance control, and recycling. Precambrian Res 104(1–2):77–93

Deepthy R, Balakrishnan S (2005) Climatic control on clay mineral formation: evidence from weathering profiles developed on either side of the Western Ghats. J Earth Sys Sci 114(5):545–556

Dutta PK (1983) The role of climate in the evolution ofdetrital and authigenic mineralogy in sandstone from the Gondwana Supergroup, India [unpublished. Ph.D. thesis]: Bloomington, Indiana University, p 169

Fan JX, Shen SZ, Erwin DH, Sadler PM, MacLeod N, Cheng QM, Zhao YY (2020) A high-resolution summary of Cambrian to early Triassic marine invertebrate biodiversity. Science 367:272–277

Fedo CM, Wayne Nesbitt H, Young GM (1995) Unraveling the effects of potassium metasomatism in sedimentary rocks and paleosols, with implications for paleoweathering conditions and provenance. Geology 23(10):921–924

Fielding CR, Frank TD, Isbell JL (2008) Resolving the Late Paleozoic ice age in time and space. Geological Society of America, Boulder, p 441

Garzanti E, Resentini A (2016) Provenance control on chemical indices of weathering (Taiwan river sands). Sediment Geol 336:81–95

Garzanti E, Andó S, France-Lanord C, Censi P, Vignola P, Galy V, Lupker M (2011) Mineralogical and chemical variability of fluvial sediments 2. Suspended-load silt (Ganga–Brahmaputra, Bangladesh). Earth Planet Sci Lett 302(1–2):107–120

Garzanti E, Padoan M, Setti M, López-Galindo A, Villa IM (2014) Provenance versus weathering control on the composition of tropical river mud (southern Africa). Chem Geol 366:61–74

Ghose NC, Mukherjee D, Chatterjee N (2005) Plume generated Mesoproterozoic mafic-ultramafic magmatism in the Chotanagpur mobile belt of eastern Indian shield margin. J Geol Soc India 66(6):725

Ghosh SC (2002) The raniganj coal basin: an example of an Indian Gondwana rift. Sediment Geol 147(1–2):155–176

Ghosh S, Sarkar S (2010) Geochemistry of Permo–Triassic mudstone of the Satpura Gondwana basin, central India: Clues for provenance. Chem Geol 277(1–2):78–100

Ghosh S, Sarkar S, Ghosh P (2012) Petrography and major element geochemistry of the Permo–Triassic sandstones, central India: implications for provenance in an intracratonic pull-apart basin. J Asian Earth Sci 43(1):207–224

Ghosh SC, Nandi A, Ahmed G, Roy DK (1996) Study of Permo–Triassic boundary in Gondwana sequence of Raniganj Basin. In: Proc. IXth International Gondwana Symposium Oxford and IBH Pub., New Delhi, Calcutta, pp 195–206

Ghosh S, Mukhopadhyay J, Chakraborty A (2019) Clay Mineral and Geochemical Proxies for Intense Climate Change in the Permian Gondwana Rock Record from Eastern India. Research, p 8974075

Gu XX, Liu JM, Zheng MH, Tang JX, Qi L (2002) Provenance and tectonic setting of the Proterozoic turbidites in Hunan, South China: geochemical evidence. J Sediment Res 72(3):393–407

Guo Y, Yang S, Su N, Li C, Yin P, Wang Z (2018) Revisiting the effects of hydrodynamic sorting and sedimentary recycling on chemical weathering indices. Geochim Cosmochim Ac 227:48–63

Guo Y, Yang S, Deng K (2021) Disentangle the hydrodynamic sorting and lithology effects on sediment weathering signals. Chem Geol 586:120607

Guo Y, Li Y, Deng K, Wang Z, Yang S (2024) Decoding the signals of sediment weathering: toward a quantitative approach. Chem Geol 651:122009

Hardy RG, Tucker ME (1988) X-ray powder diffrac-tion of sediments. In: Tucker ME (ed) Techniques in sedimentology. Blackwell Scientific Publications, London, pp 191–228

Harker A (2011) The natural history of igneous rocks. Cambridge University Press, Cambridge, p 454

Harnois L (1988) The CIW index: a new chemical index of weathering. Sediment Geol 55(3):319–322

Hayashi KI, Fujisawa H, Holland HD, Ohmoto H (1997) Geochemistry of~ 1.9 Ga sedimentary rocks from northeastern Labrador, Canada. Geochim Cosmochim Acta 61:4115–4137

Hieronymus B, Kotschoubey B, Boulègue J (2001) Gallium behaviour in some contrasting lateritic profiles from Cameroon and Brazil. J Geochem Explor 72:147–163

Hu J, Li Q, Fang N, Yang J, Ge D (2015) Geochemistry characteristics of the Low Permian sedimentary rocks from central uplift zone, Qiangtang Basin, Tibet: insights into source-area weathering, provenance, recycling, and tectonic setting. Arab J Geosci 8:5373–5388

Hundert T, Piper DJ, Pe-Piper G (2006) Genetic model and exploration guidelines for kaolin beneath unconformities in the Lower Cretaceous fluvial Chaswood Formation, Nova Scotia. Explor Min Geol 15(1–2):9–26

Isbell JL, Henry LC, Gulbranson EL, Limarino CO, Fraiser ML, Koch ZJ, Dineen AA (2012) Glacial paradoxes during the late Paleozoic ice age: evaluating the equilibrium line altitude as a control on glaciation. Gondwana Res 22(1):1–19

Jurikova H, Gutjahr M, Wallmann K, Flögel S, Liebetrau V, Posenato R, Eisenhauer A (2020) Permian-Triassic mass extinction pulses driven by major marine carbon cycle perturbations. Nat Geosci 13(11):745–750

Kaila KL (1986) Tectonic framework of Narmada-Son lineament—a continental rift system in central India from deep seismic soundings. Reflect Seismol Glob Perspect 13:133–150

Laskar B (1979) Evolution of Gondwana coal basin. In: Laskar B, Raja- Rao CS (eds) Fourth International Gondwana Symposium. Hindustan Publishing Corporation, Delhi, pp 223–237

Lin NH, Guo Y, Wai SN, Tamehe LS, Wu Z, Naing NM, Zhang J (2019) Sedimentology and geochemistry of Middle Eocene-Lower Oligocene sandstones from the western Salin Sub-Basin, the Central Myanmar Basin: Implications for provenance, source area weathering, paleo-oxidation and paleo-tectonic setting. J Asian Earth Sci 173:314–335

Mahadevan TM (2002) Geology of Bihar and Jharkhand. GSI Publications 2(1)

Mazumder R, Van Loon AJ, Mallik L, Reddy SM, Arima M, Altermann W, De S (2012) Mesoarchaean-Palaeoproterozoic stratigraphic record of the Singhbhum crustal province, eastern India: a synthesis. Geol Soc Lond Spec Publ 365(1):31–49

McLennan SM (1993) Weathering and global denudation. J Geol 101(2):295–303

McLennan SM (2001) Relationships between the trace element composition of sedimentary rocks and upper continental crust. Geochem Geophys Geosyst 2:1021–1024

McLennan SM, Ross Taylor S (2011) Geology, geochemistry and natural abundances. In: Encyclopedia of inorganic and bioinorganic chemistry

Mehta DRS (1956) A revision of the geology and coal resources of the Raniganj Coalfield. Geol Surv India Mem 84:113

Mitra ND (1994) Tensile resurgence along fossil sutures: a hypothesis on the evolution of Gondwana basins of peninsular India. In: Proceedings of 2nd Symposium on Petroliferous Basins of India, pp 55–62

Mongelli G, Critelli S, Perri F, Sonnino M, Perrone V (2006) Sedimentary recycling, provenance and paleoweathering from chemistry and mineralogy of Mesozoic continental red bed mudrocks, Peloritani Mountains, Southern Italy. Geochem J 40(2):197–209

Moore DM, Reynolds RC (1989) X-ray diffraction and the identification and analysis of clay minerals. Oxford University Press (OUP), Oxford

Moradi AV, Sarı A, Akkaya P (2016) Geochemistry of the Miocene oil shale (Hançili Formation) in the Çankırı-Çorum Basin, Central Turkey: Implications for Paleoclimate conditions, source–area weathering, provenance and tectonic setting. Sediment Geol 341:289–303

Mukhopadhyay G, Mukhopadhyay SK, Roychowdhury M, Parui PK (2010) Stratigraphic correlation between different Gondwana basins of India. J Geol Soc India 76(3):251–266

Murthy S, Chakraborti B, Roy MD (2010) Palynodating of subsurface sediments, Raniganj Coalfield, Damodar Basin, West Bengal. J Earth Syst Sci 119:701–710

Nabbefeld B, Grice K, Twitchett RJ, Summons RE, Hays L, Böttcher ME, Asif M (2010) An integrated biomarker, isotopic and palaeoenvironmental study through the Late Permian event at Lusitaniadalen. Spitsbergen Earth Planet Sci Lett 291(1–4):84–96

Nagarajan R, Armstrong-Altrin JS, Kessler FL, Jong J (2017) Petrological and geochemical constraints on provenance, paleoweathering, and tectonic setting of clastic sediments from the Neogene Lambir and Sibuti Formations, northwest Borneo. In Sediment provenance, pp 123–153

Naqvi SM, Rao VD, Narain H (1974) The protocontinental growth of the Indian shield and the antiquity of its rift valleys. Precambrian Res 1(4):345–398

Nesbitt H, Young GM (1982) Early Proterozoic climates and plate motions inferred from major element chemistry of lutites. Nature 299(5885):715–717

Nesbitt HW, Young GM (1984) Prediction of some weathering trends of plutonic and volcanic rocks based on thermodynamic and kinetic considerations. Geochim Cosmochim Acta 48(7):1523–1534

Nesbitt HW, Young GM (1989) Formation and diagenesis of weathering profiles. J Geol 97(2):129–147

Nesbitt HW, Young GM (1996) Petrogenesis of sediments in the absence of chemical weathering: effects of abrasion and sorting on bulk composition and mineralogy. Sedimentology 43(2):341–435

Parker A (1970) An index of weathering for silicate rocks. Geol Mag 107(6):501–504

Pascoe EW (1956) A manual of the geology of India and Burma: manager of publications, Gov't. of India, New Delhi

Patel RC, Sinha HN, Anupam Kumar B, Singh P (2014) Basin provenance and post-depositional thermal history along the continental P/T boundary of the Raniganj basin, eastern India: constraints from apatite fission track dating. J Geol Soc India 83(4):403–413

Perri F (2020) Chemical weathering of crystalline rocks in contrasting climatic conditions using geochemical proxies: an overview. Palaeogeogr Palaeoclimatol Palaeoecol 556:109873

Ratcliffe K, Wright M, Montgomery P, Palfrey A, Vonk A, Vermeulen J, Barrett M (2010) Application of chemostratigraphy to the Mungaroo Formation, the Gorgon field, offshore northwest Australia. APPEA J 50:371–388

Roddaz M, Viers J, Brusset S, Baby P, Hérail G (2005) Sediment provenances and drainage evolution of the Neogene Amazonian foreland basin. Earth Planet Sci Lett 239(1–2):57–78

Roddaz M, Viers J, Brusset S, Baby P, Boucayrand C, Hérail G (2006) Controls on weathering and provenance in the Amazonian foreland basin: Insights from major and trace element geochemistry of Neogene Amazonian sediments. Chem Geol 226(1–2):31–65

Roddaz M, Debat P, Nikiéma S (2007) Geochemistry of Upper Birimian sediments (major and trace elements and Nd–Sr isotopes) and implications for weathering and tectonic setting of the Late Paleoproterozoic crust. Precambrian Res 159(3–4):197–211

Roser BP, Korsch RJ (1986) Determination of tectonic setting of sandstone-mudstone suites using SiO_2 content and K_2O/Na_2O ratio. J Geol 94(5):635–650

Rudnick R, Gao S (2003) Composition of the continental crust. In: Rudnick RL (ed), The Crust. In: Holland HD, Turekian KK (eds), Treatise on Geochemistry, vol 3. Elsevier–Pergamon, Oxford, pp 1–64

Saha AK (1994) Crustal evolution of Singhbhum north Orissa eastern India. Mem Geol Soc India

Saikia A, Gogoi B, Ahmad M, Ahmad T (2014) Geochemical constraints on the evolution of mafic and felsic rocks in the Bathani volcanic and volcano-sedimentary sequence of Chotanagpur Granite Gneiss Complex. J Earth Syst Sci 123(5):959–987

Sangeeta A, Kingson O, Yadav BS, Pandey N, Meitei NR (2023) Geochemistry of the siliciclastic sediments in the Barak basin, Indo-Burma Range, India: Insights into provenance, paleoclimate, and depositional history. J Asian Earth Sci: X 10:100161

Sanyal S, Sengupta P (2012) Metamorphic evolution of the Chotanagpur granite gneiss complex of the east Indian shield: current status. Geol Soc Spec Publ 365(1):117–145

Sarkar A, Yoshioka H, Ebihara M, Naraoka H (2003) Geochemical and organic carbon isotope studies across the continental Permo–Triassic boundary of Raniganj Basin, eastern India. Palaeogeogr Palaeoclimatol Palaeoecol 191(1):1–14

Sawant SS, Kumar KV, Balaram V, Rao DS, Rao KS, Tiwari RP (2017) Geochemistry and genesis of craton-derived sediments from active continental margins: insights from the Mizoram Foreland Basin, NE India. Chem Geol 470:13–32

Sengupta S, Sarkar G, Ghosh Roy AK, Bhaduri SK, Gupta SN, Mandal A (2000) Geochemistry and Rb-Sr geochronology of acid tuffs from the northern fringe of the Singhbhum craton and their significance in the Precambrian evolution. Indian Minerals, p 54

Sharma KM, Ezcurra M, Tiwari RP, Patnaik R, Singh YP, Singh NA (2024) Additional information on the archosauriforms from the lowermost Triassic Panchet Formation of India and the affinities of "Teratosaurus (?) bengalensis." Public Electrón Asoc Paleontol Argent 24(1):97–107

Sheldon ND, Tabor NJ (2009) Quantitative paleoenvironmental and paleoclimatic reconstruction using paleosols. Earth-Sci Rev 95:1–52

Shen J, Feng Q, Algeo TJ, Li C, Planavsky NJ, Zhou L, Zhang M (2016) Two pulses of oceanic environmental disturbance during the Permian-Triassic boundary crisis. Earth Planet Sci Lett 443:139–152

Sindhuja CS, Manikyamba C, Pahari A, Santosh M, Tang L (2021) Metallogenesis and depositional environment of the Archean-Proterozoic carbonaceous phyllites from the Dharwar Craton, India. Ore Geol Rev 131:103966

Singh YP, Kingson O, Sharma KM, Ghosh P, Patnaik R, Tiwari RP, Pattanaik JK, Pankaj K, Herald T, Singh NP, Singh NA (2022) Evolution of the Permo–Triassic Satpura Gondwana Basin, Madhya Pradesh, India: insights from geochemical provenance and palaeoclimate of the siliciclastic sediments. Geol J 58(2):700–721

Song Y, Liu Z, Meng Q, WangY ZG, Xu Y (2017) Petrography and geochemistry characteristics of the lower Cretaceous Muling Formation from the Laoheishan Basin, Northeast China: implications for provenance and tectonic setting. Mineral Pet 111(3):383–397

Suttner LJ, Dutta PK (1986) Alluvial sandstone composition and paleoclimate; I, Framework Mineralogy. J Sediment Res 56(3):329–345

Taheri A, Jafarzadeh M, Armstrong-Altrin J, Mirbagheri SR (2018) Geochemistry of siliciclastic rocks from the Shemshak Group (Upper Triassic-Middle Jurassic), northeastern Alborz, northern Iran: implications for palaeoweathering, provenance, and tectonic setting. Geol Q 62(3):522–535

Taylor SR, McLennan SM (1985) The continental crust: its composition and evolution. Blackwell Scientific, Oxford, London, Edinburgh, Boston, Palo Alto, Melbourne, p 312

Thiry M (2000) Palaeoclimatic interpretation of clay minerals in marine deposits: an outlook from the continental origin. Earth Sci Rev 49(1–4):201–221

Verma SP, Armstrong-Altrin JS (2013) New multi-dimensional diagrams for tectonic discrimination of siliciclastic sediments and their application to Precambrian basins. Chem Geol 355:117–133

Verma SP, Armstrong-Altrin JS (2016) Geochemical discrimination of siliciclastic sediments from active and passive margin settings. Sediment Geol 332:1–12

Wanas HA, Abdel-Maguid NM (2006) Petrography and geochemistry of the Cambro-Ordovician Wajid Sandstone, southwest Saudi Arabia: Implications for provenance and tectonic setting. J Asian Earth Sci 27(4):416–429

Wanas HA, Assal EM (2021) Provenance, tectonic setting and source area-paleoweathering of sandstones of the Bahariya Formation in the Bahariya Oasis, Egypt: an implication to paleoclimate and paleogeography of the southern Neo-Tethys region during Early Cenomanian. Sediment Geol 413:105822

Wang W, Zhou MF, Yan DP, Li JW (2012) Depositional age, provenance, and tectonic setting of the Neoproterozoic Sibao Group, southeastern Yangtze Block, South China. Precambrian Res 192:107–124

Wang C, Wang Q, Chen G, He L, Xu Y, Chen L, Chen D (2017) Petrographic and geochemical characteristics of the lacustrine black shales from the Upper Triassic Yanchang Formation of the Ordos Basin, China: implications for the organic matter accumulation. Mar Pet Geol 86:52–65

Wang Z, Wang J, Fu X, Feng X, Wang D, Song C, Yu F (2018) Provenance and tectonic setting of the Quemoco sandstones in the North Qiangtang Basin, North Tibet: Evidence from geochemistry and detrital zircon geochronology. Geol J 53(4):1465–1481

Wang P, Du Y, Yu W, Algeo TJ, Zhou Q, Xu Y, Qi L, Yuan L, Pan W (2020) The chemical index of alteration (CIA) as a proxy for climate change during glacial-interglacial transitions in Earth history. Earth-Sci Rev 201:103032

Wani H, Mondal MEA (2011) Evaluation of provenance, tectonic setting, and paleoredox conditions of the Mesoproterozoic-Neoproterozoic basins of the Bastar craton, Central Indian Shield: using petrography of sandstones and geochemistry of shales. Lithosphere 3(2):143–154

Weaver CE (1967) Potassium, illite and the ocean. Geochim Cosmochim Acta 31(11):2181–2196

Xiong Z, Li T, Algeo T, Nan Q, Zhai B, Lu B (2012) Paleoproductivity and paleoredox conditions during late Pleistocene accumulation of laminated diatom mats in the tropical West Pacific. Chem Geol 334:77–91

Zhang F, Romaniello SJ, Algeo TJ, Lau KV, Clapham ME, Richoz S, Anbar AD (2018) Multiple episodes of extensive marine anoxia linked to global warming and continental weathering following the latest Permian mass extinction. Sci Adv 4(4):e1602921

Zhu Z, Liu Y, Kuang H, Benton MJ, Newell AJ, Xu H, Zhai Q (2019) Altered fluvial patterns in North China indicate rapid climate change linked to the Permian-Triassic mass extinction. Sci Rep 9(1):16818